Linnaeus University Dissertations
No 380/2020

Andreas Briggert

Modelling and strength grading of structural timber and glulam lamellae on the basis of optical scanning and dynamic excitation

Linnaeus University Press

Modelling and strength grading of structural timber and glulam lamellae on the basis of optical scanning and dynamic excitation

Linnaeus University Dissertations

No 380/2020

Modelling and strength grading of structural timber and glulam lamellae on the basis of optical scanning and dynamic excitation

Andreas Briggert

LINNAEUS UNIVERSITY PRESS

Modelling and strength grading of structural timber and glulam lamellae on the basis of optical scanning and dynamic excitation
Doctoral Dissertation, Department of Building Technology, Linnaeus University, Växjö, 2020

ISBN: 978-91-89081-47-5 (print), 978-91-89081-48-2 (pdf)
Published by: Linnaeus University Press, 351 95 Växjö
Printed by: Holmbergs, 2020

Abstract

Briggert, Andreas (2020). *Modelling and strength grading of structural timber and glulam lamellae on the basis of optical scanning and dynamic excitation,* Linnaeus University Dissertations No 380/2020, ISBN: 978-91-89081-47-5 (print), 978-91-89081-48-2 (pdf).

Machine strength grading of sawn timber is a sawmill process in which density, modulus of elasticity (MOE) and bending or tensile strength are predicted such that the timber can be assigned to strength classes. The predictions of these properties are performed using one or several so-called indicating properties (IPs), which represent a board property, or combination of board properties, measured non-destructively. A limitation of today's strength grading is that the IPs applied in the industry for prediction of strength, in general, are based on rather weak statistical relationships between IPs and strength properties, which in turn results in poor material utilisation.

It is well known that the strength of sawn timber is associated with the presence of knots and their surrounding fibre disorientations. Local fibre direction at surfaces of softwood can be determined by means of the light scattering that occur when a wood surface is illuminated by a dot-laser, i.e. by application of the so-called tracheid effect. Lately, IPs based on such measurements have been developed, and some of the suggested IPs have a strong statistical relationship to bending strength.

The purposes of the research presented in this thesis are to contribute with knowledge of possibilities and limitations of the tracheid effect and of data of fibre directions in the vicinity of knots, to evaluate if information of fibre directions at surfaces of Norway spruce sawn timber can be used to achieve a better material utilisation of glulam lamellae and finger-jointed timber, and to provide insight regarding the grading regulations in Europe.

Results presented herein show that knots and fibre direction within the interior of boards can be modelled on the basis of data obtained by means of the tracheid effect, but also that a previously proposed method to determine out-of-plane fibre angles gives poor accuracy.

As regards grading of glulam lamellae, an IP based on fibre directions and dynamic MOE is proposed for prediction of tensile strength. The latter is used when grading glulam lamellae. Application of the proposed IP resulted in substantially increased yield in strength classes. It is also shown that this IP is applicable for boards with sawn as well as with planed surface finish. Regarding current regulations for machine strength grading in Europe, results indicate that grading based on global board properties give higher yield than what is appropriate.

Keywords: Fibre direction, finger joint, machine strength grading, knots, tracheid effect, Norway spruce

To my beloved family

Acknowledgement

The research presented in this thesis was carried out at the Department of Building Technology, Faculty of Technology at Linnaeus University, Växjö, Sweden. The research was funded by the Faculty, the Knowledge Foundation, the Södra Foundation for Research and the Centre for Building and Living with Wood (CBBT), which are hereby gratefully acknowledged.

I wish to express my gratitude to several persons who have supported me these past years. Firstly, to my supervisors, Professor Anders Olsson and Senior Lecturer Dr Jan Oscarsson, thank you for trusting in me and guiding me. Both of you are true sources of inspiration, and I am extremely grateful to have had both of you as my supervisors.

Secondly, to my colleagues at the department, thank you for all research presentations, discussions and collaborations these past years. A special thanks to my previous PhD colleague, Dr Min Hu, and research engineer Bertil Enquist for good collaboration in the research lab.

I also want to express my gratitude to Martin Bacher at Microtec and Rune Ziethén at RISE, thank you for helping me and answering all my questions. Patrik Ljungdahl, Håkan Murevärn and Tomas Blomberg at WoodEye, thank you for assisting me over the years with your knowledge. I also want to express my gratitude to the former staff at Rörvik Myresjö Timber and to the staff at Södra Timber, Derome and Vida for collaboration and generous contributions in joint research projects.

Finally, to my dear family, thank you for trusting in me and supporting me. It has been hard work, but you have all been there motivating me. William and Molly, I am extremely grateful to be your father, you are the joy of my life and the best kids a father could ask for. Michaela, my wife to be, thank you for all that you have done over these last years. I would not have made this without you.

Växjö 2020-03-16

Andreas Briggert

Appended papers

Paper I — Briggert, A., Olsson, A. & Oscarsson, J. (2016). *Three-dimensional modelling of knots and pith location in Norway spruce boards using tracheid-effect scanning.* European Journal of Wood and Wood Products, 74: 725 − 739.

Paper II — Hu, M., Briggert, A., Olsson, A., Johansson, M., Oscarsson, J. & Säll, H. (2018). *Growth layer and fibre orientation around knots in Norway spruce: a laboratory investigation.* Wood Science and Technology, 52: 7 − 27.

Paper III — Briggert, A., Hu, M., Olsson, A. & Oscarsson, J. (2018). *Tracheid effect scanning and evaluation of in-plane and out-of-plane fiber direction in Norway spruce timber.* Wood and Fiber Science, 50(4): 411 − 429.

Paper IV — Briggert, A., Olsson, A. & Oscarsson, J. (2020). *Prediction of tensile strength of sawn timber: Definitions and performance of indicating properties based on surface laser scanning and dynamic excitation.* Submitted to Materials and Structures, accepted for publication.

Paper V — Briggert, A., Olsson, A. & Oscarsson, J. (2020). *Prediction of tensile strength of sawn timber: Models for calculation of yield in strength classes.* Submitted to Materials and Structures, under review.

Paper VI — Olsson, A, Briggert, A & Oscarsson, J. (2019). *Increased yield of finger jointed structural timber by accounting for grain orientation utilizing the tracheid effect.* European Journal of Wood and Wood Products, 77: 1063 − 1077.

Author's contribution to appended papers

Paper I	Andreas Briggert planned the study in collaboration with co-authors, created the model, conducted the analysis and wrote the manuscript, with input from the co-authors.
Paper II	Andreas Briggert participated in planning the study. Andreas Briggert carried out the experiments together with Min Hu and gave input on the manuscript.
Paper III	Andreas Briggert participated in planning the study. Andreas Briggert and Min Hu carried out the experiments. Andreas Briggert carried out the analysis and wrote the paper with input from the co-authors.
Paper IV	Andreas Briggert planned the study in collaboration with the co-authors, performed the data collection, conducted the analysis and wrote the manuscript with input from the co-authors.
Paper V	Andreas Briggert planned the study in collaboration with the co-authors, performed the data collection, conducted the analysis and wrote the manuscript with input from the co-authors.
Paper VI	Andreas Briggert collected data, contributed with algorithms for the modelling and gave input on the manuscript.

Contents

1 Introduction

1.1 Background

It is well known that the levels of the greenhouse gas carbon dioxide (CO_2) in the atmosphere has increased since humans started to use fossil fuels to produce energy. In November in the year 1958, the monthly average level of CO_2 in the atmosphere at Mauna Loa observatory in Hawaii was just above 313 parts per million (ppm), see Figure 1. At the same location, in the same month in 2019, the monthly average of CO_2 in the atmosphere was 410 ppm (NOAA 2020). The increased level of CO_2 in the atmosphere has resulted in a rise of the earth's average global temperature followed by melting of glaciers and polar ice caps and subsequent sea-level rise. If the average global temperature continues to increase with the same rate as today, it can lead to the collapse of ecosystems, extinction of certain animal and plant species, harsher weather such as more frequent and more severe tropical storms. To avoid such environmental changes, members of the United Nations agreed in 2015 to keep the average global temperature rise well below 2 degrees Celsius (United Nations 2015). To fulfil this aim, the emissions of greenhouse gases need to decrease considerably in the near future.

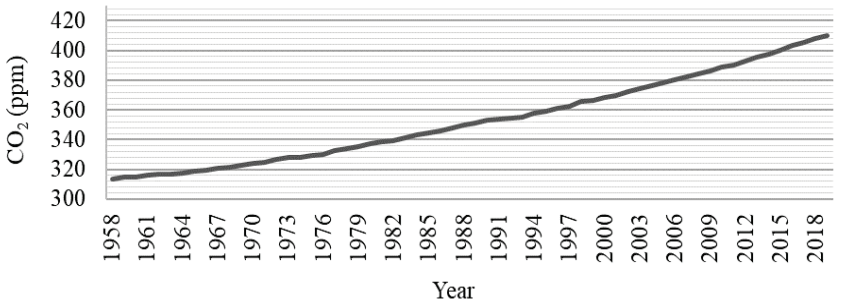

Figure 1: Average levels of CO_2 in the atmosphere at Mauna Loa observatory, Hawaii, in November in 1958 – 2019 (NOAA 2020).

The global annual emission of CO_2 in 2017 was 36 billion tonnes (Ritchie & Roser 2020). The building and construction sector accounts for approximately 40 % of these emissions (Dodoo 2019). In Europe, in the same year, the annual emission of CO_2 was 6 billion tonnes (Ritchie & Roser 2020). Here, the building and construction sector accounts for roughly 36 % of the CO_2 emissions (Bonakdar et al. 2014). The emission of CO_2 from the building and construction sector must be reduced if the average global temperature rise shall be kept below 2 degrees Celsius. A possibility to achieve a part of such a reduction is to use wood as construction material, when feasible, instead of concrete and steel, whose respective manufacturing industries emit large amounts of CO_2 in the production of the materials (Worrell et al. 2001; Price et al. 2002).

For more than one hundred years, the forest sector has been one of Sweden's most important industries. Sweden has a total land area of 41 million hectares, and 70 % of this area is covered by forests. Every year 1 % of the forest is harvested, and around 80 % of the products are exported (Swedish Forest Industries 2020). Sweden is one the of world's largest exporter of pulp, paper and sawn timber. In 1985, forests corresponding to a total volume over bark (VOB), i.e. trunk volume including bark, of 63 millions were harvested in Sweden, see Figure 2 (The Swedish Forest Agency 2020). Since then the volume of harvested forest has increased slightly almost every year, and in 2017 a total VOB of 92.5 millions were harvested. Figure 2 shows a peak in 2005; this was the year when the storm Gudrun hit Sweden and felled trees corresponding to a total VOB of approximately 75 million in one night.

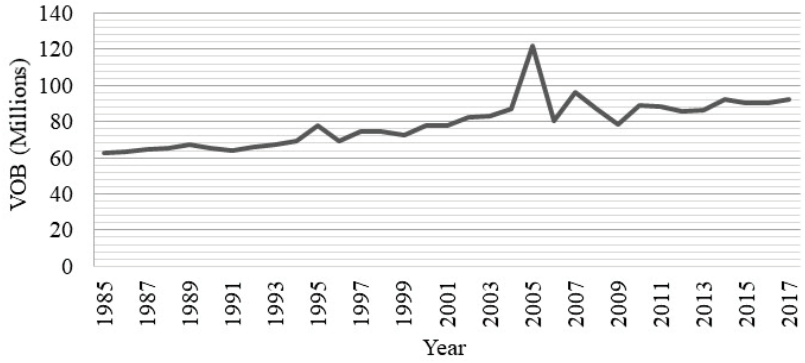

Figure 2: Annual harvesting of forest in Sweden (The Swedish Forest Agency 2020).

The most common tree species in Swedish forests are the conifers Norway spruce (*Picea abies*) and Scots pine (*Pinus sylvestris*), which constitute for approximately 41 % and 39 % of the forests, respectively. The remaining 20 % consists of deciduous trees such as birch (*Betula pubescens* & *Betula pendula),* and beech *(Fagus sylvatica)* among others.

Wood is a product of nature and includes abnormalities such as knots, reaction wood, top ruptures, bark pockets and decay. Many of these abnormalities are in standing trees necessary for their survival. For example, the arrangement of fibres in a branch-stem junction, i.e. a knot, differs considerably from fibre arrangements in other parts of the stem (Foley 2003; Müller et al. 2015; Shigo 1985). In such a junction, fibres are organised so that the tree can fulfil necessary transportation of nutrients and water between stem and branch, and such that the junction can resist the stresses that are caused by the load of the branch. Another example is reaction wood. Conifers continuously exposed to strong wind loads or growing in a slope produce a type of reaction wood called compression wood at the compression side of the stem, especially in the lower part of trees (Dinwoodie 2000). This type of wood is produced so that the tree can resists the compression stresses that are developed in a stem under such conditions. Compression wood can also be found below branches. Deciduous trees grown under similar conditions instead produce a type of reaction wood called tension wood on the tension side of the stem.

Many of the abnormalities necessary for a tree's survival in nature are in wood products such as sawn timber considered as defects, since the occurrence of such abnormalities generally decrease a board's strength and stiffness. For example, Johansson (2003) evaluated results from 1800 sawn timber boards tested in bending or tension and concluded that more than 90 % of the failures were associated with the presence of knots. Since there is a natural variety of abnormalities such as knots, both with respect to number and size, in each individual board, sawn timber used for structural purposes need to be graded, i.e. the mechanical properties of each individual piece need to be predicted.

Wood is generally considered as an orthotropic material, which means that mechanical properties such as strength and modulus of elasticity (MOE) differ between three mutually perpendicular directions. These directions are referred to as longitudinal, radial and tangential direction. The longitudinal direction in this coordinate system follows the length direction of the fibres. In clear wood, i.e. in parts of a log where the fibre direction is not affected by knots or other abnormalities, this length direction is, in general, close to being parallel with the stem direction. However, small deviations occur due to spiral grain and taper of the log. The radial direction is defined as the transverse length direction of the fibres that follow the direction from pith to bark in the stem and the tangential direction as the transverse length direction of the fibres that follow the direction of the circumference of the stem. The mechanical properties of the radial and tangential directions are in engineering contexts usually not separated. As a result, strength and MOE are defined as parallel to fibres or perpendicular to fibres. The tensile strength parallel to fibres is roughly $30-50$ times higher than across the fibres (Thelandersson 2003), whereas the compression strength parallel to fibres is about $15-25$ times higher than across the fibres (Johansson 2011). For small straight-grained, defect-free specimens,

i.e. clear wood, the correlation between strength and MOE is high. For example, Foslie (1971) found for Norway spruce clear wood a coefficient of determination (r^2) of 0.76 between bending strength and MOE in bending. This correlation is lower for sawn timber, mainly due to the occurrence of abnormalities such as knots. For sawn timber of Norway spruce, coefficients of determination of 0.53 − 0.72 between bending strength and MOE in bending are reported (Johansson 2003; Olsson & Oscarsson 2017).

Some type of assessment of the mechanical properties in a piece of wood has most likely been performed ever since humans started to use wood for structural purposes. However, the first guidelines for developing grading rules for prediction of a board's mechanical properties were published in 1927 in the American Society for Testing and Materials (ASTM) Standard D245 (Madsen 1992), and in the 1930s, similar grading rules were introduced in several countries around the world. At this time, grading was carried out by means of visual inspection, i.e. boards were examined visually by a human to ensure that certain visible defects did not exceed the limits specified in the grading rules (Johansson 2003). The first grading rules in Sweden, the so-called T-rules, was published in 1951. The weaknesses of visual grading are, however, obvious. When visually examining a board, only defects visible on the surface, such as knot types, knot surface areas and annual ring widths at the end cross-sections, can be taken into consideration. Other defects influencing the mechanical properties such as density and local fibre direction cannot be taken into account. Visual grading is still in use, and a diversity of different visual strength grading rules exist. In the Nordic countries, visual grading is carried out in accordance with INSTA 142 (SIS 2010).

In the United States and Australia at the end of the 1950s, the idea of using non-destructive measurements, obtained by application of machines, for grading of sawn timber was introduced (Madsen 1992). The purpose of this idea was to develop grading methods aiming at a more efficient and accurate utilisation of available wood materials. The first machine grading methods were based on the relationship that exists between a board's flatwise stiffness, determined by a three-point bending setup, and edgewise bending strength. The stiffness, represented by a calculated MOE, is in such a setup determined as

$$E_{\text{flat}} = \frac{PL^3}{48Iw} \tag{1}$$

where P is the load, which is applied in the middle of the span between the two supports, L is the length of the span, I is the board's second moment of inertia and w the deflection at the middle of the span where the load P is applied. The first grading machines for commercial use employing a three-point bending setup were the *Microstress Grading Machine*, the *Continuous Lumber Tester* and the *Stress-O-Matic Grading Machine*. The *Microstress Grading Machine*

was introduced in Australia around 1960s (Galligan & McDonald 2000), whereas the *Continuous Lumber Tester* and *Stress-O-Matic Grading Machine* were approved for commercial use in the United States in 1962 (ALSC 2020). The first grading machine in Sweden was approved in 1974 (Johansson et al. 1992), and was of make *Computermatic*. In this machine, a load was applied in three-point bending in a board's weak direction by a roller and kept constant while the deflection was continuously recorded as a board passed through the machine in the board's longitudinal direction. The largest value of the deflection of each board was then used to grade the boards to different strength classes (Johansson & Claesson 1989). As regards machine strength grading of sawn timber, methods based on three-point bending dominated the sawmill industry up until the beginning of the 2000s (Oscarsson, 2014), and such methods are still in use.

In the late 1990s, a strength grading method based on dynamic excitation was introduced. In this method, the axial dynamic MOE is used for prediction of a board's bending or tensile strength, MOE and even density. For a board with ideal free-free boundary conditions, the axial dynamic MOE is calculated as

$$E_{\mathrm{dyn,n}} = 4\rho\left(\frac{f_{\mathrm{a,n}} L_{\mathrm{tot}}}{n}\right)^2 \tag{2}$$

where ρ is the board density, $f_{\mathrm{a,n}}$ is the axial resonance frequency corresponding to the n^{th} mode of vibration and L_{tot} is the length of the board (Ohlsson & Perstorper 1992). The axial resonance frequencies of a board can be determined by inducing a longitudinal vibration by a hammer blow at one of the board ends while simultaneous measuring either the oscillation with a laser vibrometer or the sound transmitted through the vibrating board using a microphone. The measurement result is then converted to the frequency domain using Fast Fourier Transform. Usually, the axial resonance frequency corresponding to the first mode of vibration is applied in *Eq. 2*. Examples of machines applying the axial dynamic MOE for prediction of mechanical properties are Precigrader of make Dynalyse and Viscan Plus of make Microtec. In 2019, this grading method was utilized in more than 70 % of the grading machines used in Swedish sawmills (RISE 2019).

A strength grading method using X-ray was also introduced in the late 1990s. X-ray scanning of boards provide high-resolution density data in two dimensions and since the density of knots is roughly twice as high as the surrounding clear wood density (Schajer 2001), such data enable knot dimensions to be used in grading methods. However, details of how this local density data is applied for prediction of strength and MOE is not, in general, made public by the manufacturers. The first grading machines based on X-ray and approved for commercial use in Europe was the EuroGrecomat-702 of

make Microtec. Today, there are approved strength grading methods combining data from both X-ray scanning and dynamic excitation (Bacher 2008).

In the 2010s, strength-grading methods based on information of in-plane fibre direction at the longitudinal surfaces were approved for use on the European market. In such methods, the in-plane fibre directions, i.e. the direction of the fibres along the surface of the board, are measured by means of the so-called *tracheid effect,* which can be explained as follows. When a wood surface is illuminated by high-intensity light, such as light from a dot-laser, some of the light will directly be reflected at the surface, whereas another part of the light will penetrate the surface and scatter within the wood before it is reflected from the surface. Softwood species like Norway spruce conduct such high-intensity light better in the fibres longitudinal direction than in their transverse directions. As a result, the shape of the reflected light will resemble an ellipse. The major axis of such an ellipse is oriented in the same direction as a projection of the fibres length direction onto the surface, see Figures 3a − b. The first grading method based on application of the tracheid effect and approved for commercial use on the European market was developed by Olsson et al. (2013). In this method, measured in-plane fibre directions on board surfaces and axial dynamic MOE are used to calculate local bending MOEs along the longitudinal direction of the board. The lowest determined local bending MOE along the board is then used to predict the bending strength of the board. Examples of grading machines, using the tracheid effect and approved for commercial use in Europe, are the WoodEye Strength Grader of make WoodEye and the RS-StrengthGrader of make Rema Sawco.

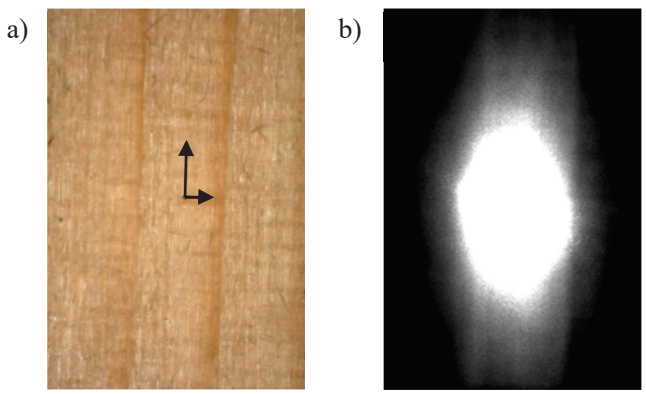

Figure 3: a) Clear wood surface of Norway spruce. b) Spread of laser light on the surface displayed in a) when illuminated by a dot-laser. The lengths and directions of the arrows displayed in a) illustrate the magnitude and the directions of the minor and the major axis of the ellipse in b), respectively.

Sawn timber is graded to strength classes using three so-called grade determining properties (GDPs). The GDPs are density, MOE and bending or tensile strength. The latter depends on the application; bending strength is considered when grading structural timber, and tensile strength when grading glulam lamellae. Bending and tensile strength are the GDPs that are most difficult to predict, see for example, Olsson and Oscarsson (2017). Machine strength grading methods can, therefore, partially be evaluated by means of its accuracy to predict strength. For a complete evaluation of a strength grading method, it is also advisable to calculate and compare yield in different strength classes. Hanhijärvi and Ranta-Maunus (2008) evaluated different machine strength grading methods by comparing their accuracy to predict strength. For this purpose, they used measurement results from almost 1400 boards of Norway spruce and more than 900 boards of Scots pine. A selection of coefficients of determination between applied indicating properties (IPs) and bending or tensile strength obtained for Norway spruce in this study are given in Table 1. An IP is a board property or combination of board properties that is used in a statistical model to predict one or several GDPs, see *Section 3.3.1. Indicating property*. Furthermore, Table 1 also includes the r^2 between the IP defined in Olsson et al. (2013) and bending strength obtained for a sample of more than 900 Norway spruce boards (Olsson & Oscarsson 2017). A comparison of the results indicates that the method based on data from surface laser scanning and dynamic excitation gives the most accurate prediction of bending strength, and that the method based on data from X-ray scanning and dynamic excitation gives the most accurate prediction of tensile strength. However, two things should be noted. Firstly, the coefficients of determination cited from Hanhijärvi and Ranta-Maunus (2008) are comparable since the same sample of boards was used for all calculation. Conclusions based on a comparison between results from different investigation should be drawn with caution since the evaluation is carried out using different samples. Secondly, before the present thesis work was carried out, the method based on fibre direction and dynamic excitation had not been evaluated for tensile strength.

Table 1: Coefficients of determinations for four different grading methods.

Grading method	Results from:	Bending strength r^2	Tension strength r^2
Flatwise MOE in bending	Hanhijärvi & Ranta-Maunus (2008)	0.54	0.58
Axial dynamic MOE	Hanhijärvi & Ranta-Maunus (2008)	0.57	0.58
X-ray + axial dynamic MOE	Hanhijärvi & Ranta-Maunus (2008)	0.64	0.64
Fibre direction + axial dynamic MOE	Olsson & Oscarsson (2017)	0.69	-

Several research groups in Europe have contributed in the field of machine strength grading in the last few years, by suggesting new models for timber and methods for grading, and by discussions and critical assessment of current standards for grading. For example, Sarnaghi and van de Kuilen (2019) and Jenkel and Kaliske (2018) both have suggested methods for prediction of tensile strength using finite element modelling based on knot reconstruction in combination with flow grain analogy (e.g. Goodmann & Bodig 1980). Viguier et al. (2015) proposed a method for prediction of bending strength based on data from both surface laser scanning and X-ray scanning. Lukacevic et al. (2015) suggested methods, based on this kind of data, for prediction of both bending and tensile strength. As regards discussion and critical assessment of currents standards for grading, Ridley-Ellis et al. (2016) gave a thorough explanation/discussion of the machine strength grading regulations in Europe, whereas Rais and van de Kuilen (2015) presented results indicating issues that should be considered in future versions of the grading standards.

1.2 Research objectives

The intention of the research presented in this thesis is to contribute to the long-term goal aiming at a more efficient use of sawn timber as a construction material by development of accurate strength grading methods. Development of such methods, however, requires both a profound understanding and accurate interpretation of measurement results, appropriate mechanical and material models based on such data and definitions of accurate IPs. Therefore, the objectives of the research presented in this thesis are to

1) contribute with knowledge of possibilities and limitations of the tracheid effect, i.e. investigate if useful information other than knowledge of the in-plane fibre direction can be obtained/determined by means of the tracheid effect,

2) determine the fibre orientation in three dimensions (3D) in the vicinity of knots and evaluate non-destructive methods for determination of such fibre orientation,

3) evaluate if information of fibre directions at surfaces of sawn timber of Norway spruce can be used for accurate grading and better material utilisation of glulam lamellae, i.e. derive and evaluate an IP to tensile strength based on such data,

4) evaluate if information of fibre directions at surfaces of sawn timber of Norway spruce can be used to decrease waste in the production of finger-jointed structural timber, and

5) provide insight into the grading regulations in Europe, regarding conditions using IPs based on global or local properties of boards, respectively.

These five objectives are discussed in the six papers attached to this thesis. Objectives 1 and 2 relate to papers I − III. Objectives 3 and 4 relate to papers IV and VI, respectively, whereas objective 5 is dealt with in paper V.

1.3 Methodology and Limitations

The scientific methods applied in the work presented in papers I – IV and VI can be described as hypothetico-deductive since their purposes can be formulated in terms of hypotheses that could be falsified. As regards paper V, the investigation is more of inductive type since conclusions were drawn on the basis of measurement results without any predetermined hypothesis. This does not mean, however, that the findings presented in this paper were unexpected since they to some extent are in line with results presented in previous research.

A limitation of this thesis is that all investigations and measurements were carried out on a single softwood species, namely Norway spruce. The presented results are, therefore, only valid for this kind of wood. However, since many softwood species have similar structures, results presented herein give an indication for other species as well.

2. Wood – mechanical properties and density

2.1 Clear wood

2.1.1 Microscopic structure

Wood mainly consists of three elements, namely carbon (C), oxygen (O) and hydrogen (H). These three elements form the molecular chains of cellulose, hemicellulose and lignin. In addition, wood includes small amounts of nitrogen (N), minerals and extractives. The latter is a collective name for several different chemical compounds such as waxes, fats and resins. In Norway spruce, the proportion of cellulose, hemicellulose and lignin are 42 ± 2 %, 27 ± 2 % and 28 ± 3 %, respectively, (Dinwoodie 2000). Chains of cellulose placed side-by-side and embedded in a matrix of hemicellulose and lignin, form a microfibril.

In softwood species, two types of cells are present in greater numbers. These are called tracheids, herein also referred to as fibres, and parenchymas. The former is the most common cell type in Norway spruce (>90 %), and these cells have a length of 2 – 4 mm and a width of approximately 30 μm (Havimo et al. 2008). About 90 % of the tracheids are vertically aligned in a stem; small deviations occur due to spiral grain and tapering of the stem. The main functions of tracheids are to support the tree and to transport nutrients and water, whereas the purpose of the parenchymas, which are located in the horizontal rays, is to provide storage of food materials.

The tracheid cell wall consists of three different parts: the middle lamella, the primary wall and the secondary wall, see Figure 4 (Dinwoodie 2000; Johansson 2011; Persson 2000; Säll 2002). The middle lamella is the outermost layer which is mainly composed of lignin, and serves as an adhesive between tracheid cells. The primary wall is located between the middle lamella and the secondary wall and it consists of randomly orientated microfibrils. The secondary wall occupies the largest proportion of the total cell wall and it is the part of the wall that is decisive for the mechanical properties of wood.

In the secondary wall, three different layers are observed. These are usually denoted S_1, S_2 and S_3. The S_1-layer includes approximately 10 % of the entire cell wall thickness (Fengal & Stoll 1973). In this layer, the microfibrils follow both a clockwise and a counterclockwise spiral up the cell, and the length direction of the microfibrils deviate considerably from the tracheid's length direction. The angle between the length direction of a tracheid and the microfibrils within its cell wall is called the microfibril angle (MFA). Brändström et al. (2003) measured the MFA in the S_1-layer in Norway spruce specimens by means of both an electron microscope and a light microscope and

concluded that the MFA is about 70 – 90˚ in this layer. Other studies, based on X-ray diffraction analysis, report MFAs of 50 – 70˚ (Dinwoodie 2000; Paakkari & Serimaa 1984).

About 80 % of the entire cell wall thickness consists of the S_2-layer (Brändström 2001; Dinwoodie 2000; Fengal & Stoll 1973). In this layer, the length direction of microfibrils follow a counterclockwise spiral up the cell, see Figure 4, and the MFA is between 5 – 40˚ (Kantola & Kähkönen 1963; Kantola & Seitsonen 1969; Paakkari & Serimaa 1984; Saranpää et al. 1998). The MFA in this layer tends to be in the lower part of the interval in tracheids close to the bark and in the upper range in tracheids close the pith.

The remaining part of the cell wall consists of the S_3-layer. This is the part of the cell wall that is directly adjacent to the lumen. Results from different investigations show that the MFA varies between 10 – 90˚ and the microfibrils follow both clockwise and counterclockwise spirals up the cell (Brändström 2001; Dinwoodie 2000; Paakkari & Serimaa 1984).

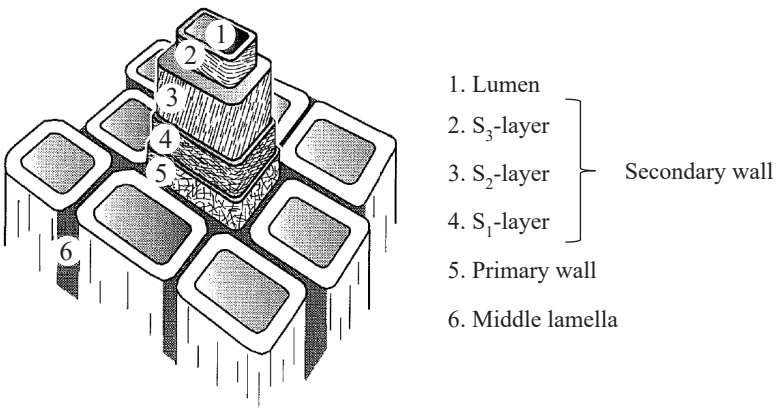

Figure 4: Cell wall structure of a tracheid/fibre. Figure originates from Persson (2000).

2.1.2 Macroscopic structure

2.1.2.1 Earlywood and latewood

Tree growth occurs by means of cell division in tissues called meristems. Longitudinal tree growth, i.e. the primary growth, occurs in apical meristems located in shoots and roots, and radial growth, i.e. the secondary growth, in lateral meristems located at the cork cambium and the vascular cambium, see Figure 5. The cork cambium produces outer bark, whereas the vascular cambium produces xylem and phloem. The xylem is the part of the tree that is located on the inside of the vascular cambium, i.e. the part of the stem including what is commonly called wood. The phloem is part of the inner bark and is located between the vascular cambium and the outer bark. Organic molecules

are transported in the phloem, whereas water and dissolved minerals are transported in xylem called sapwood. Xylem that no longer carries out such transportation of water and dissolved minerals is called heartwood.

Softwood species, like Norway spruce, grow in a seasonal sequence, and two distinct zones can be identified of each year's growth: earlywood and latewood, see Figure 5. At the beginning of a growth period, the need for conduction of water and dissolved minerals within the stem of a standing tree is large. Therefore, trees produce fibres with thin cell walls and large lumens, and such fibres form the earlywood. Later on, as the growth rate slows down, the need for water and dissolved mineral conduction decreases. Then, trees start to produce fibres that have thicker cell walls and smaller lumens. This type of wood is called latewood. Because of its thicker cell walls and smaller lumens, the density of latewood is larger than the density of earlywood. For Norway spruce, at a 12 % moisture content (MC), the density of latewood is between 650 – 775 kg/m^3, whereas the density of earlywood is 375 – 525 kg/m^3 (Saranpää 2003). Earlywood and latewood areas can be identified by their coloration. Earlywood is generally brighter than latewood because of the thin cell walls and large lumens.

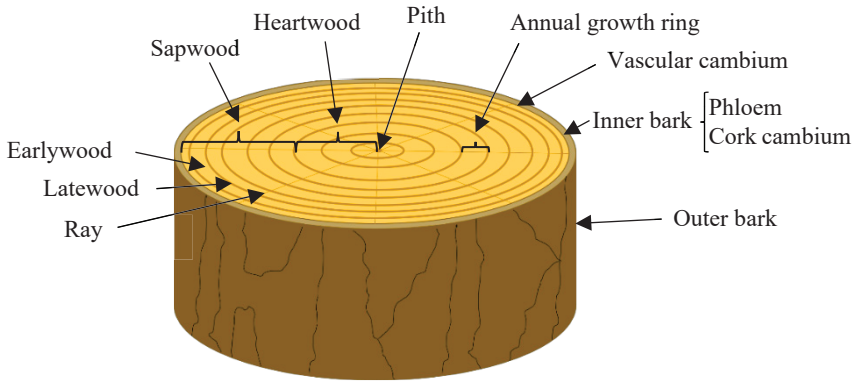

Figure 5: Structure of a softwood stem.

2.1.2.2 Annual growth rings

An annual growth ring, also called annual ring, consists of the earlywood and the latewood produced during one growth season. The width in the radial direction of the stem including the earlywood and the latewood produced in one year is called annual ring width, see Figure 5. The amount of wood produced in a tree during a specific year depends on the tree's genetics, silvicultural methods, and local climate conditions on the plant site such as soil quality, amount of precipitation, sunlight exposure and temperature. As regards the latter, in years when the local climate conditions are favourable, the growth rate of trees is increased and the annual rings become wider than years when local climate conditions are less favourable. In Norway spruce, higher growth rate

results in an increased percentage of earlywood and thus decreased density. This is not the case for all wood species. For example, an increased growth rate in oak (*Quercus*) results in a higher portion of latewood, which in turn results in an increased density (Dinwoodie 2000).

Furthermore, regarding the relationship between growth rate and density, it is not always such that wood from the trees of Norway spruce with small annual ring widths have a higher density than trees with large annual ring widths. At the northern latitudes, tree growth is restricted by the short summers and trees do not produce as much latewood as trees grown at more southern latitudes. Consequently, trees from northern latitudes have a higher proportion of earlywood, which in turn results in a decreased density, even if the ring widths are small. As regards silvicultural methods, an important factor for tree growth is the stand density. Generally, a high stand density results in smaller annual ring widths since trees in such stands get less sunlight and need to share the water and nutrients available in the ground.

2.1.2.3 Spiral grain

The length direction of the fibres is not perfectly in line with the length direction of the stem. Generally, the length direction of the fibres follows a spiral around the circumference of the stem. Young trees of Norway spruce produce fibres that follow a clockwise spiral up the stem, and, in most cases, the largest inclination of the fibres to the length direction of the stem, also called spiral grain angle, occurs between annual rings 4 – 10, counted from the pith and outwards (Säll 2002). In succeeding annual rings, the spiral grain angle usually decreases, and within annual rings 40 – 70 the fibres are almost vertically directed. Fibres produced in more mature trees (approximately from annual ring 70 and higher) instead tend to follow a counterclockwise spiral up the stem.

2.1.3 Density and mechanical properties of clear wood

2.1.3.1 Density

Clear wood density varies between species. The density of the cell wall, on the other hand, is approximately 1500 kg/m^3 for all wood species (Kollmann & Côte 1968). The density of clear wood in Norway spruce depends on the proportion of earlywood and latewood within each annual ring, MC, presence of extractives etcetera.

The presence of moisture in wood influences its mass. An increased amount of moisture, i.e. a higher MC, results in an increased mass. Likewise, if the amount of moisture is reduced, the mass is decreased. The volume of a wood specimen also depends on the MC. Below the fibre saturation point (FSP), which in Norway spruce occurs at a MC of approximately 30 %, moisture is absorbed/desorbed by the cell walls which in turn leads to an increased/decreased volume of these walls, and consequently to swelling/shrinking of the specimen. No such swelling/shrinking occurs above

the FSP since additional moisture then become free water within the cell lumen. Mass and volume of a piece of wood must therefore be determined at a measured MC when these quantities are applied for calculation of density. The density of Norway spruce is generally quoted at an MC of 12 %, which corresponds to the equilibrium MC when such wood is conditioned at a relative humidity of 65 % and a temperature of 20˚ Celsius. The clear wood density at 12 % MC is, in accordance with EN 408 (2010) and EN 384 (2016), calculated as

$$\rho_{12\%} = \frac{m}{Lhb}\left(1 - \frac{1}{200}\cdot(\mu - 12)\right) \tag{3}$$

where m, L, h and b are the specimen's mass, length, width and thickness, respectively, and μ is the MC at the time of the measurements. Note that direct use of *Eq. 3* only is applicable if the specimen has the shape of a cuboid. Otherwise, if the specimen has an irregular shape, the volume (Lhb) must be determined by, for example, the water displacement method.

The clear wood density varies within a stem. For example, Steffen et al. (1997) showed that the density of clear wood specimens from mature trees of Norway spruce varies from about 400 to 600 kg/m^3 from pith to bark at an MC of 12 %, i.e. wood from the outer parts of trees have a higher density than wood produces in the earlier years of the growth of a tree.

The density of a specimen of clear wood has a rather high correlation to both strength and MOE. For small defect-free specimens of Norway spruce, Foslie (1971) found coefficients of determination between clear wood density and bending strength, and between clear wood density and MOE in bending, of 0.66 and 0.64, respectively.

2.1.3.2 Modulus of elasticity

When a wood sample is loaded in bending, compression or tension, the instantaneous deformations are approximately proportional to the size of the applied load up to the so-called limit of proportionality. For a clear wood specimen loaded in tension, the limit of proportionality occurs at about 60 % of the specimen's tensile strength. For small clear wood specimens loaded in compression, the limit of proportionality occurs at 30 – 50 % of the specimen's compression strength (Dinwoodie 2000). Below the limit of proportionality, the material behavior is linearly elastic and relationship between stresses and strains is determined by the MOE.

As mentioned in *Section 1.1 Background*, wood is generally considered as an orthotropic material and represented by the longitudinal (L), radial (R) and tangential (T) directions, which are mutually perpendicular to each other, see Figure 6. It is well known that the MOE parallel to the fibres length direction, i.e. the L-direction, is high compared to the MOEs in the fibres transverse

directions, i.e. the *R*- and *T*-directions. In clear wood of Norway spruce, at 12 % MC, the MOE is typically about 10 700 MPa in the *L*-direction, and about 710 MPa and 430 MPa, respectively, in the *R*- and *T*-directions (Dinwoodie 2000), but large variations occur, see next paragraph. The MOEs in these directions can be estimated by loading specimens of clear wood, i.e. straight-grained, defect-free specimens, while simultaneously measuring displacements and then determine the linear relationship between calculated stresses and strains using Hooke's law.

In clear wood specimens, the MOE depends on the MFA and density, but also on other factors such as MC and temperature. For example, an increased MFA in the S_2-layer results in a decreased MOE in the *L*-direction and vice versa. Furthermore, specimens with higher density usually have higher MOEs than specimens with low density. Regarding MC, above the FSP, the MOE is generally regarded as independent of MC. However, below the FSP, a decrease of the MC results in an increase of the MOE, and, consequently, an increase of the MC results in a decrease of the MOE. A literature review of existing studies carried out in the 80's showed that the MC has a stronger effect on the MOE in the *R*- and *T*-directions than in the *L*-direction (Gerhards 1982). As regards temperature, the MOEs decrease with increasing temperature and vice versa.

When the MOE is determined for a small specimen of clear wood, the MOE also depends on, just as for the density, the specimen's origin within the stem. Steffen et al. (1997) determined the MOE in the *L*-direction of small specimens of Norway spruce and concluded that the MOE increases from about 10 000 MPa in specimens cut close the pith to approximately 22 000 MPa in specimens cut close to the bark.

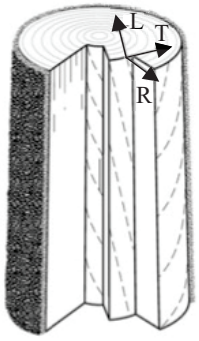

Figure 6: Illustration of the LRT coordinate system in relation to a piece of a log. Figure originates from Ormarsson (1999).

2.1.3.3 Strength

Just as for MOE, the strength of wood is directional dependent. The tensile strength in clear wood is approximately 30 − 50 times higher parallel to the fibres, i.e. in the *L*-direction, than in the perpendicular directions, i.e. *R* and *T*-

directions (Thelandersson 2003). The compressive strength is about 15 − 25 times higher in the length direction of the fibres than in their perpendicular directions (Johansson 2011). This anisotropic behavior can, according to Dinwoodie (2000), partly be explained by the bonds of the microfibrils. In the length direction of the microfibrils, the bonds are covalent whereas the bonding between microfibrils in the transverse length direction are of hydrogen type. Hydrogen bonds are weaker than covalent bonds and thus easier to break. As a result, a higher strength is obtained in the length direction of the fibres than in their perpendicular directions.

The strength of wood also depends on density and MFA. The strength increases with increasing density, and an increased MFA in the S_2-layer results in a reduced strength in the *L*-direction. Furthermore, and as for the MOE, the strength also depends on the environmental conditions such as MC and temperature.

Both in directions parallel and perpendicular to fibres, pure tensile tests show that the stress-strain relationship is almost linear up to failure, which means that tensile failures are brittle. In pure compression tests, on the other hand, failure is often more ductile and large plastic strains evolve after the limit of proportionality has been reached.

This far, only strength in orthogonal directions parallel and perpendicular to fibres have been discussed. However, by means of the well-known Hankinson's formula (Hankinson 1921), it is possible to estimate, for an arbitrary direction (i.e. a direction with an angle θ to the fibre direction) the strength by

$$f(\theta) = \frac{f_{\mathrm{L}} f_{\mathrm{T}}}{f_{\mathrm{L}} \sin^{n}(\theta) + f_{\mathrm{T}} \cos^{n}(\theta)} \tag{4}$$

where f_{L} is the strength in the fibre direction, f_{T} is the strength in the direction perpendicular to the fibres and n is an empirically determined constant; for tension $n \approx 1.5 - 2$, and for compression $n \approx 2 - 2.5$.

2.2 Sawn timber

2.2.1 Defects in sawn timber

2.2.1.1 Knots and their surrounding fibre orientation

Branches are directed from the pith and outwards in the stem's radial direction, see Figure 7a. The branch-stem junction consists of an alternating pattern of fibres grown around the branch in the length direction of the stem and fibres grown from the stem into the branch (Foley 2003; Shigo 1985). This rather complex system of interlocking fibre pattern gives the junction its strength and enables transportation of water and nutrients between the branch and the stem.

Generally, sawn timber of Norway spruce include knots, and as mentioned earlier, the presence of such defects are decisive for the mechanical properties of boards. The decrease in strength and stiffness, associated with the presence of knots, are determined by their positions and sizes, but also on the surrounding fibre distortion.

Knots are generally categorised on the basis of their visual appearance on the wood surface. For example, the wide faces of a timber board cut as illustrated in Figure 7a display knot surfaces that are cut perpendicular to the length direction of the branch, see Figure 7b. Such knot surfaces are, based on its shape, categorised as either a round knot or an oval knot. If the ratio between the major and the minor axis of such a knot is smaller than 1.5, the knot surface is defined as a round knot, otherwise it is defined as an oval knot (Casselbrandt et al. 2000). Rotation of the indicated board illustrated in Figure 7a by 90˚ around an axis parallel to the length direction of the stem would result in the display of a splay knot on one of the wide faces of the board (or even on both of them if the board thickness is smaller than the diameter of the knot). An example of the latter is shown in Figure 7c. Knots are also categorised by the condition of the knot. For example, a live knot, i.e. a growing branch, is called a sound knot whereas a knot that no longer grows is called a dead knot.

To quantify the occurrence of knots in boards, for the purpose of grading, different knot measures have been proposed, but knot measures alone are poor predictors of the mechanical properties. For example, Johansson (1976) evaluated five different knot measures and for the so-called TKAR measure (area of the projection of all knots within a length of 150 mm on the cross-section, divided by the full cross-sectional area), coefficients of determination of 0.26 and 0.35 for bending and tensile strength, respectively, were obtained.

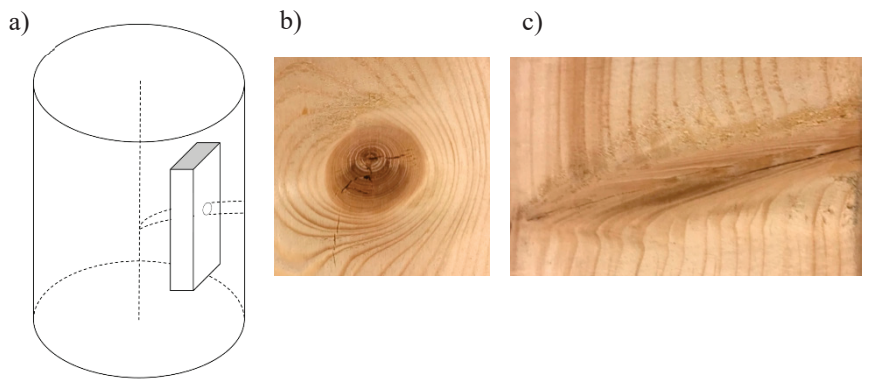

Figure 7: a) Illustration of a stem including a part of a board. The vertical dashed line in the centre of the stem represents the pith of the log, whereas the dashed lines drawn outwards in the stem's radial direction represents a branch. b) Wood surface including a round knot and c) a splay knot.

2.2.1.2 Top rupture

The top part in a young standing tree sometime breaks when exposed to either large external loads such as wind and snow or browsing game. Such a failure is called a top rupture. When a top rupture occurs, the top branches in the standing part of the tree start to bend and grow upwards. A shoot of one of these branches will eventually replace the previous leading shoot. As the tree continues to grow, and the circumference of the tree increases, the branch with the leading shoot is eventually overgrown and included in the stem. Such a natural replacement of a broken top of a tree cause severe fibre distortion within the stem.

The fibre distortion caused by a top rupture can have a strong influence on both strength and stiffness. A top rupture is, however, unlike knots, only present in a limited area in a few stems, and thus occurs less frequently in sawn timber.

2.2.1.3 Reaction wood

Trees grown on a slope or continuously exposed to strong wind loads develop a type of wood called reaction wood to preserve vertical growth. In deciduous trees, such wood is formed on the tension side of the stem (tension wood), whereas in conifers the reaction wood is formed on the compression side of the stem (compression wood).

The latewood fibres in compression wood are generally shorter, rounder and have thicker cell walls than the fibres present in normal latewood, and the wood itself has a larger proportion of latewood in the annual rings (Isaksson 1999). As a result, compression wood has a higher density than normal wood. Furthermore, the MFA in the S_2-layer is larger than the corresponding MFA in the S_2-layer in fibres present in normal wood (Côté et al. 1967), and in severe compression wood, the S_3-layer is missing (Johansson 2011).

Compression wood is characterised by its high compression strength, low tensile strength and low MOE, and when loaded to its maximum capacity, the failures are generally more brittle than failures in normal wood. Areas including compression wood can often be identified visually by the latewood's dark and brownish colour.

2.2.2 Density and mechanical properties of sawn timber

2.2.2.1 Density

In addition to the physical characteristics influencing the density of clear wood such as different proportions of earlywood and latewood etcetera, sawn timber also includes defects such as knots and reaction wood. This results in a difference in board density between boards, and also a local density variation along each board's length, width and thickness. Local densities, as a mean value across the thickness, can be determined using X-ray scanning (Bacher 2008). Such scanning gives basis for a two-dimensional density plot. An example of

such a plot of a board of Norway spruce originating from southern Sweden is shown in Figure 8a. The nominal cross-sectional dimensions of this board were 50 × 150 mm. In this figure, blue colour corresponds to clear wood whereas red and yellow correspond to knots and their transition zones. The local densities obtained by X-ray scanning can further be used to calculate the mean density of each cross-section, see Figure 8b. For this particular board, the local densities of each cross-section varied between just below 400 kg/m^3 to just above 550 kg/m^3. The higher densities in this interval were obtained for cross-sections including knots. The board density of a particular board can be determined as the mean of all its local densities.

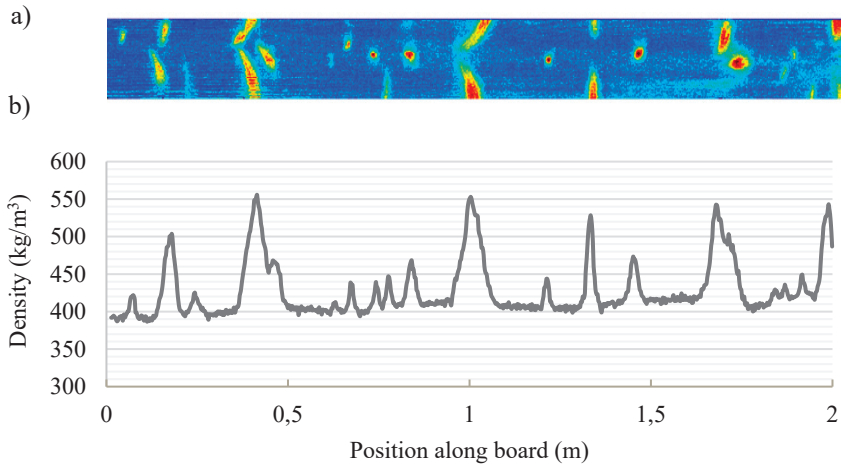

Figure 8: a) Two-dimensional density plot, and b) mean density for each cross-section of the part of the board displayed in a). Data were obtained using the X-ray scanner Goldeneye of make Microtec.

It was mentioned in *Section 2.1.3.1 Density* that rather high coefficients of determinations are obtained between clear wood density and clear wood bending strength (r^2 = 0.66) and between clear wood density and clear wood MOE in bending (r^2 = 0.64). However, since strength and stiffness of timber boards largely depend on the occurrence of knots and their related fibre direction disorientation, which lead to decreased stiffness and strength, density is usually a rather poor indicator of strength and stiffness in sawn timber. For Norway spruce, as can be seen in Table 2, coefficients of determination obtained in different studies between board density and bending strength are in the range of 0.16 − 0.40, and between board density and tensile strength in the range of 0.18 − 0.38. Table 2 also includes coefficients of determination between board density and board stiffness, the latter represented by static local MOE in bending and tension, respectively, see EN 408 (2010).

Table 2: Coefficients of determination, obtained in different studies of Norway spruce, between board density and strength, and between board density and MOE. The numbers in the table head refer to the following investigations: 1: Johansson et al. (1992), 2: Hoffmeyer (1984), 3: Hoffmeyer (1990), 4: Lackner et al. (1988), 5: Glos et al. (1982), 6: Johansson (1976), 7: Olsson & Oscarsson (2017) and 8: enclosed paper IV. Results from investigation 1 – 6 are also compiled in Johansson (2003).

	Coefficients of determination							
	Board density							
Source	1	2	3	4	5	6	7	8
Tensile strength	0.38				0.29	0.38		0.19
MOE in tension								0.45
Bending strength	0.16	0.30	0.16	0.40			0.16	
MOE in bending							0.27	

2.2.2.2 Stiffness

The stiffness of sawn timber is usually expressed in terms of a calculated MOE, and, as for the density, the stiffness varies along boards due to different proportion of earlywood and latewood, position and size of knots and other defects. Generally, a board's longitudinal tensile stiffness is expressed in terms of a static MOE in tension (E_t), which, in accordance with EN 408 (2010), is calculated as

$$E_t = \frac{l_1\left(F_2 - F_1\right)}{A\left(u_2 - u_1\right)} \tag{5}$$

where $F_2 - F_1$ is a load increment between two points on the straight-line portion of the load-displacement curve, u_1 and u_2 are deformations, i.e. the relative displacements over the span l_1, at F_1 and F_2, respectively and A is the cross-sectional area of the board. The deformations shall, in accordance with EN 408 (2010), be determined over a length l_1 of 5 times the larger cross-sectional dimension (i.e. h). The distance between the grips of the testing machine must be at least $9h$, and deformation measurements shall not be carried out closer than $2h$ to the ends of the grips. Furthermore, the tested length shall include the anticipated weakest cross-section, i.e. the cross-section at which failure is expected to occur. If this is not achievable, it is permitted to test the second weakest cross-section (EN 384, clause 5.2). An illustration of the test setup applied for the determination of a board's static MOE in tension is shown in Figure 9.

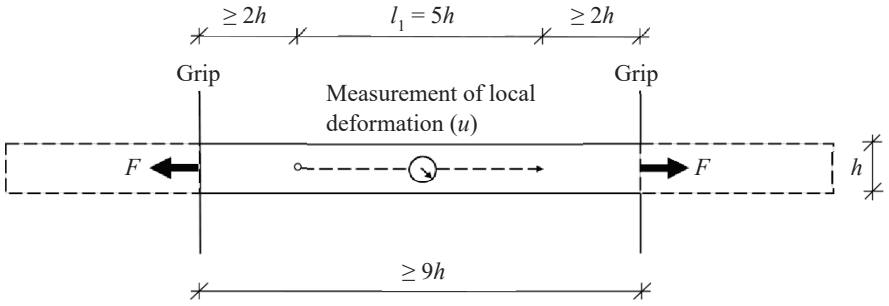

Figure 9: Test setup in accordance with EN 408 (2010) for determination of stiffness and strength of a board tested in tension.

In bending, two stiffness measures are defined in EN 408 (2010). Both are determined using the four-point bending test setup exhibited in Figure 10 and they are referred to as MOEs in bending. The stiffness measures are the static edgewise local MOE ($E_{m,local}$) and static edgewise global MOE ($E_{m,global}$), which are calculated, respectively, as

$$E_{m,local} = \frac{a l_2^2 \left(P_2 - P_1\right)}{16 I \left(v_2 - v_1\right)} \tag{6}$$

and

$$E_{m,global} = \frac{l_3^3 \left(P_2 - P_1\right)}{b h^3 \left(w_2 - w_1\right)} \left[\left(\frac{3a}{4l_3} \right) - \left(\frac{a}{l_3} \right)^3 \right] \tag{7}$$

where a is the distance between the loading positions and the closest support (a = $6h \pm 1.5h$), l_2 and l_3 are the spans for determination of local MOE ($5h$) and the distance between the supports ($18h \pm 3h$), respectively, P_1 and P_2 are the total loadings at two load levels on the straight-line portion of the load-displacement curve, I is the second moment of inertia (i.e. $bh^3/12$ for a rectangular cross-section), v_1 and v_2 are the deflections measured over the span of $5h$ at load levels P_1 and P_2, respectively, and w_1 and w_2 are the deflections measured over the total length between the supports at load levels P_1 and P_2, respectively. Furthermore, the length between loading positions shall include the anticipated weakest cross-section (or second weakest cross-section) (EN 384, clause 5.2).

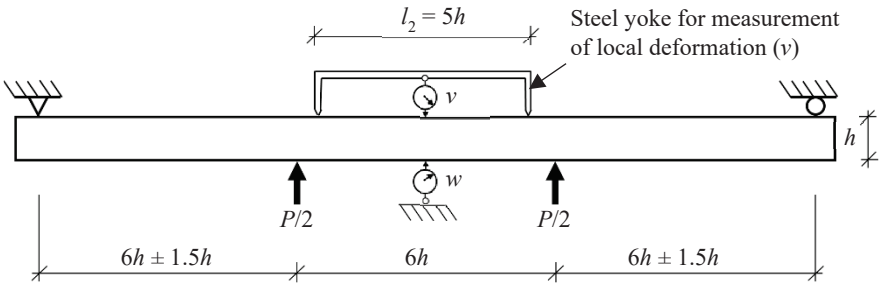

Figure 10: Test set up in accordance with EN 408 (2010) for determination of stiffness and strength of a board tested in bending. Figure originates from Oscarsson (2014).

The stiffness measures E_t, $E_{m,local}$ and $E_{m,global}$ at a reference MC of 12 % are, in accordance with EN 384 (2016), calculated as

$$E_{x,12\%} = E_x \left(1 + \frac{1}{100}(\mu - 12)\right) \tag{8}$$

where E_x represents either E_t, $E_{m,local}$ or $E_{m,global}$ and μ is the board's MC at the time of testing, which, according to EN 408 (2010), can be determined using a full cross-section specimen, free of knots and resin pockets, cut from the board. In accordance with EN 384 (2016), *Eq. 8* is valid for MC between $8\,\% \leq \mu \leq 18\,\%$. Application of *Eq. 8* implies that E_t, $E_{m,local}$ or $E_{m,global}$ are increased or decreased by 1 % for every 1 % difference between the MC of a board at the time of testing and the reference MC of 12 %. The MOE in the length direction of the board at a 12 % MC, usually referred to as MOE parallel to the grain, are estimated, in accordance with EN 384 (2016), as

$$E_{t,0} = E_{t,0,12\%} \tag{9}$$

or

$$E_{m,0} = E_{m,local,12\%} \tag{10}$$

or

$$E_{m,0} = E_{m,global,12\%} \cdot 1.3 - 2690 \tag{11}$$

where $E_{m,global,12\%}$ is defined in MPa.

Stiffness measures, expressed in terms of MOEs as defined above, generally correlate stronger to strength than what density does. For sawn timber of Norway spruce, such stiffness measures result in coefficients of determination of $0.53 - 0.72$ for bending strength, and coefficients of determinations of $0.48 - 0.70$ for tensile strength, see Table 3.

Table 3: Coefficients of determination, obtained in different studies of Norway spruce, between MOE and strength. The numbers in the table head refer to the same investigations as referred to in Table 2.

	Coefficients of determination MOE in bending ($E_{m,0}$) or tension ($E_{t,0}$)							
Source	1	2	3	4	5	6	7	8
Tension strength	0.70				0.69	0.58		0.48
Bending strength	0.72	0.53	0.55	0.56			0.62	

2.2.2.3 Strength

Generally, the strength of sawn timber is to a large degree dependent on positions and sizes of knots. Around and within knots, tension stresses perpendicular to the fibre direction are induced. The occurrence of such stresses is one important reason for failure in timber boards, since the strength perpendicular to the fibres is much lower than the strength in the direction parallel to the fibres. In accordance with EN 408 (2010), using the test set up exhibited in Figure 9, the tensile strength of a board is determined as

$$f_{t,0} = \frac{F_{max}}{A} \tag{12}$$

where F_{max} is the maximum load applied in a test. The bending strength of a board is, in accordance with the same standard, determined using the test set up displayed in Figure 10 and calculated as

$$f_{m} = \frac{3P_{max}a}{bh^2} \tag{13}$$

where P_{max} is the maximum load applied.

It is well known that the strength of a timber piece is influenced by the volume of the piece (Bohannan 1966; Isaksson 2003; Madsen & Buchanan 1986). For example, provided that the timber is of the same quality, there is a higher probability that longer boards include weaker sections than shorter ones, i.e. the so-called length effect, which leads to the fact that longer boards generally have a lower strength than shorter ones. There is also a depth effect, which means that boards with smaller depths/widths are less likely to contain

serious defects and thus more likely to have high strength. This depth effect shall, in accordance with EN 384 (2016), be considered when determining the bending or tensile strength of Norway spruce boards with a h, see Figure 9 – 10, lesser than 150 mm, by dividing the tensile or bending strength obtained by *Eqs. 12 − 13*, respectively, by a factor k_h. This factor is calculated as

$$k_h = \min \begin{cases} \left(\frac{150}{h}\right)^2 \\ 1.3 \end{cases}. \quad (14)$$

2.2.2.4 Descriptive statistics of density, MOE and strength

The arithmetic mean (mean), standard deviation (std) and coefficient of variation (CoV) of density, stiffness and strength of sawn timber of Norway spruce from the Nordic countries are given in Table 4. The results originate from Paper IV and Olsson and Oscarsson (2017). Both of these investigations each included more than 900 Norway spruce boards of different dimensions.

The bending strength is generally higher than the tensile strength (Isaksson 2003), which is confirmed by the results in Table 4. In an edgewise bending set up, the stress within the wood member varies, and the highest stresses only occur near the narrow edges within the test span. Strength-reducing defects such as knots located at the middle of the board width, or in the compression zone, may therefore have limited influence on the bending strength of the board. In tensile tests, however, high stresses are obtained over the entire volume included in the test span, and defects located anywhere within the cross-section of the board can be decisive for the tensile strength.

Table 4: Means (mean), standard deviations (std) and coefficient of variation (CoV) of density, MOE and strength for Norway spruce timber originating from the Nordic countries.

MOE measurement	Results from:	mean	std	Cov
ρ (kg/m^3)	Paper IV	447	45.3	0.10
$E_{t,0}$ (N/mm^2)	Paper IV	12 000	2700	0.22
$f_{t,0}$ (N/mm^2)	Paper IV	30.4	11.7	0.38
ρ (kg/m^3)	Olsson & Oscarsson (2017)	441	41	0.09
$E_{m,local}$ (N/mm^2)	Olsson & Oscarsson (2017)	11 600	2370	0.20
$E_{m,global}$ (N/mm^2)	Olsson & Oscarsson (2017)	11 000	1840	0.17
f_m (N/mm^2)	Olsson & Oscarsson (2017)	42.1	11.3	0.27

3. Strength grading of sawn timber in Europe

3.1 Introduction

For sawn timber, there are currently two types of strength grading systems in use in Europe: visual grading and machine grading (EN 14081-1 2016). In the former system, grading is carried out by means of visual inspection, i.e. boards are examined visually by a human or an optical scanner to ensure that certain visible defects do not exceed limits specified in the grading rules. Visual grading rules for sawn timber from the Nordic countries are given in INSTA 142 (SIS 2010).

Machine strength grading is carried out using an approved grading machine, or combination of machines, measuring one or several board properties non-destructively. The results of such measurements are used to calculate one or several IPs, and by means of predefined settings of the applied IPs, the board is then either assigned to a graded class or rejected.

Development and evaluation of a machine strength grading method consist of two parts. The first of these concerns definitions and calculations of IPs and determination of the GDPs for a sample of boards and evaluation of the statistical relationship between the IPs and the GDPs. The second part consists of determining settings for the IPs such that the minimum requirements of characteristic values of the GDPs are fulfilled when boards with IPs exceeding the determined settings are assigned to a graded class.

3.2 Strength classes

Based on its future application, sawn timber is graded as either structural timber or lamellae. Structural timber is used, for example, as joists in floors or as chords and webs in roof trusses whereas lamellae are used in glulam products. Sawn timber graded according to the visual grading rules given in INSTA 142 (SIS 2010) are assigned to T-classes (structural timber) or LT-classes (lamellae). Machine strength graded timber, on the other hand, are assigned to the strength classes defined in EN 338 (2016). Structural timber is, in accordance with the latter standard, assigned to C-classes (softwood) or D-classes (hardwood), whereas lamellae are assigned to T-classes. It should be noted that T-classes given EN 338 (2016) are not the same as the T-classes as given in INSTA 142 (SIS 2010). Design values, i.e. characteristic values, for mechanical properties and density, of a few of the T-classes and C-classes defined in EN 338 (2016) are given in Table 5 − 6, respectively.

Table 5: Design values for a few of the T-classes defined in EN 338 (2016).

	Class	T14	T18	T22	T26
Strength properties [N/mm²]					
Bending	$f_{m,k}$	20.5	25.5	30.5	35
Tension parallel	$\boldsymbol{f_{t,0,k}}$	**14**	**18**	**22**	**26**
Tension perpendicular	$f_{t,90,k}$	0.4	0.4	0.4	0.4
Compression parallel	$f_{c,0,k}$	21	23	26	28
Compression perpendicular	$f_{c,90,k}$	2.5	2.7	2.7	2.9
Shear	$f_{v,k}$	4.0	4.0	4.0	4.0
Stiffness properties [kN/mm²]					
Mean MOE parallel bending	$\boldsymbol{E_{t,0,mean}}$	**11.0**	**12.0**	**13.0**	**14.0**
5 percentile MOE parallel bending	$E_{t,0,k}$	7.4	8.0	8.7	9.4
Mean MOE perpendicular	$E_{t,90,mean}$	0.37	0.40	0.43	0.47
Mean shear modulus	G_{mean}	0.69	0.75	0.81	0.88
Density [kg/m³]					
5 percentile density	$\boldsymbol{\rho_k}$	**350**	**380**	**390**	**410**
Mean density	ρ_{mean}	420	460	470	490

Table 6: Design values for a few of the C-classes defined in EN 338 (2016).

	Class	C14	C18	C24	C30
Strength properties [N/mm²]					
Bending	$\boldsymbol{f_{m,k}}$	**14**	**18**	**24**	**30**
Tension parallel	$f_{t,0,k}$	7.2	10	14.5	19
Tension perpendicular	$f_{t,90,k}$	0.4	0.4	0.4	0.4
Compression parallel	$f_{c,0,k}$	16	18	21	24
Compression perpendicular	$f_{c,90,k}$	2.0	2.2	2.5	2.7
Shear	$f_{v,k}$	3.0	3.4	4.0	4.0
Stiffness properties [kN/mm²]					
Mean MOE parallel bending	$\boldsymbol{E_{m,0,mean}}$	**7.0**	**9.0**	**11.0**	**12.0**
5 percentile MOE parallel bending	$E_{m,0,k}$	4.7	6.0	7.4	8.0
Mean MOE perpendicular	$E_{m,90,mean}$	0.23	0.30	0.37	0.40
Mean shear modulus	G_{mean}	0.44	0.56	0.69	0.75
Density [kg/m³]					
5 percentile density	$\boldsymbol{\rho_k}$	**290**	**320**	**350**	**380**
Mean density	ρ_{mean}	350	380	420	460

3.3 Machine grading

3.3.1 Indicating property

3.3.1.1 Introduction to regression analysis

Indicating properties are fundamental for machine strength grading. The purpose of the next section, i.e. *Section 3.3.1.2 Definition of an indicating property*, is to clarify and give the general definition of an IP. However, to

prepare for this, some basic theory of regression analysis is first given in the present section.

Regression analysis is used to evaluate the statistical relationship between a set of known dependent and independent variables. The latter is also called predictor variables, and this term is used from now on. The calculation procedure is commonly known as single regression analysis (also referred to as simple regression analysis) when only one predictor variable is applied in the regression model, and as multiple regression analysis when more than one predictor variables are used. The classical linear regression model is defined as follows. Let z_1, z_2, …, z_m be a set of m predictor variables for a jth observation. The jth dependent variable (y_j) can then be defined as

$$y_j = \beta_0 + \beta_1 z_{j1} + \beta_2 z_{j2} + ... + \beta_m z_{jm} + \varepsilon_j \tag{15}$$

where β_k, $k = 0, 1, \ldots, m$, are the so-called regression coefficients and ε_j is the residual, which accounts for measurement errors and effects of other variables not considered in the model. For n observations, the regression model can be written as

$$\begin{bmatrix} y_1 \\ y_2 \\ \vdots \\ y_n \end{bmatrix} = \begin{bmatrix} 1 & z_{11} & z_{12} & \cdots & z_{1m} \\ 1 & z_{21} & z_{22} & \cdots & z_{2m} \\ \vdots & \vdots & \vdots & \ddots & \vdots \\ 1 & z_{n1} & z_{n2} & \cdots & z_{nm} \end{bmatrix} \begin{bmatrix} \beta_0 \\ \beta_1 \\ \beta_2 \\ \vdots \\ \beta_m \end{bmatrix} + \begin{bmatrix} \varepsilon_1 \\ \varepsilon_1 \\ \vdots \\ \varepsilon_n \end{bmatrix} \tag{16}$$

or in matrix notation as

$$\mathbf{Y} = \mathbf{Z}\boldsymbol{\beta} + \boldsymbol{\varepsilon} \tag{17}$$

where $\mathbf{Y}$ is an $n \times 1$ vector containing observations of the dependent variables, $\mathbf{Z}$ is an $n \times (m+1)$ matrix containing a single column of ones and the observations of all the predictor variables, $\boldsymbol{\beta}$ is an $(m+1) \times 1$ vector containing the regression coefficients, i.e. β_k, where $k = 0, 1, \ldots, m$, and $\boldsymbol{\varepsilon}$ is an $n \times 1$ vector containing the n residuals. Using a set of known predictor variables and corresponding dependent variables, the regression coefficients in $\boldsymbol{\beta}$ can be estimated. One approach to estimate the regression coefficients is to select $\boldsymbol{\beta}$ such that it minimises the sum of squared residuals (i.e. $\boldsymbol{\varepsilon}'\boldsymbol{\varepsilon}$), which typically is not zero. The approach of selecting $\boldsymbol{\beta}$ such that the sum of squared residuals is minimised is known as the least square method. The regression coefficients that minimise

the sum of squared residuals, see for example Johnson and Wichern (2013), are determined as

$$\hat{\boldsymbol{\beta}} = \left(\mathbf{Z}'\mathbf{Z}\right)^{-1}\mathbf{Z}'\mathbf{Y}. \tag{18}$$

The hat sign above $\boldsymbol{\beta}$ in *Eq. 18* is used to indicate that these regression coefficients are estimated values of the true regression coefficients. Using the estimated regression coefficients obtained from *Eq. 18* and a set of observations of the predictor variables, a predicted value of the dependent variable can now be calculated as

$$\hat{y}_{\mathrm{j}} = \hat{\beta}_0 + \hat{\beta}_1 z_{\mathrm{j1}} + \hat{\beta}_2 z_{\mathrm{j2}} + \ldots + \hat{\beta}_{\mathrm{m}} z_{\mathrm{jm}}. \tag{19}$$

The expression given in *Eq. 19* is known as the regression equation. When only one predictor variable is applied in the regression model, i.e. single linear regression is employed, the regression equation given in *Eq. 19* is reduced to

$$\hat{y}_{\mathrm{j}} = \hat{\beta}_0 + \hat{\beta}_1 z_{\mathrm{j1}}. \tag{20}$$

The quality of a linear regression model can be evaluated by means of the coefficient of determination, which is calculated as

$$r^2 = \frac{\sum_{\mathrm{i}=1}^{n}\left(\hat{y}_{\mathrm{i}} - \overline{y}\right)^2}{\sum_{\mathrm{i}=1}^{n}\left(y_{\mathrm{i}} - \overline{y}\right)^2} \tag{21}$$

where $\overline{y}$ is the arithmetic mean of the set of known dependent variables. The unitless r^2 value is between 0 and 1 and indicates the proportion of the variance in the dependent variable explained by means of the predictor variable(s). An $r^2 = 1$ thus implies that the total variance of the dependent variable is explained by means of the predictor variable(s), whereas an $r^2 = 0$ implies that there is no linear relationship between predictor and dependent variables. Furthermore, the r^2 value generally increases when the number of predictor variables is increased, even when additional predictor variables do not actually improve the model. This problem can be circumvented by using an adjusted r^2 calculated as

$$r_{adj}^2 = 1 - \frac{\left(1 - r^2\right)\left(n - 1\right)}{n - m - 1}. \tag{22}$$

where n and m are, as defined earlier, the number of observation and the number of predictor variables, respectively, and r^2 is the coefficient of determination calculated by means of *Eq. 21*. Another measurement of interest when evaluating a regression model is the standard error of estimate (*SEE*), which is calculated as

$$SEE = \sqrt{\frac{\sum_{i=1}^{n}\left(y_i - \hat{y}_i\right)^2}{n-2}}. \tag{23}$$

The *SEE* is a measure of the accuracy of the predictions made by application of the regression line as defined in *Eqs. 19 − 20*. The *SEE* is given in the same unit as the dependent variable.

3.3.1.2 Definition of an indicating property

An IP can be a determined board property such as, for example, board density or axial dynamic MOE. Determined board properties, such as those just mentioned, can also be applied as predictor variables in multiple linear regression to define an IP. A set of known dependent variables (i.e. a set of values of one of the GPDs) and predictor variables (i.e. determined board properties) are then used to estimate the regression coefficients by, for example, the least square method, see *Section 3.3.1.1 Introduction to regression analysis*. Using the obtained regression equation and a board's set of determined board properties, it is possible to predict a value of the board's dependent variable by means of *Eq. 19*. When multiple linear regression is used to combine board properties obtained by one or several grading machines, the IP is calculated using the regression equation based on the estimated regression coefficients. With reference to *Section 3.3.1.1 Introduction to regression analysis*, two possible definitions of IP are now given in Table 7.

Table 7: Definition of an IP using one or several determined board properties.

Numbers of determined board properties	Determined board properties (predictor variables)	IP
1	z_1	z_1 or $\hat{y}_j$
> 1	$z_1, z_2, \ldots, z_m$	$\hat{y}_j$

3.3.2 Settings of IPs applied in a new strength grading method

3.3.2.1 General

As mentioned earlier, machine strength grading of sawn timber is carried out by means of predefined settings for the IPs such that minimum requirements of characteristic values of the GDPs are fulfilled when boards with IPs exceeding the determined settings are assigned to a graded class. For the T-classes, the GDPs are tensile strength, MOE and density. The GDPs for the C- and D-classes are bending strength, MOE and density. The procedure for determination of settings are described in EN 14081-2 (2018), and can be divided into five main consecutive steps, namely, sampling, collection of data using the grading machine, destructive testing, derivation of settings and verification of settings.

3.3.2.2 Requirements of sampling

Settings for an IP applied in a new machine type shall be determined using at least 450 boards (EN 14081-2 2018). However, it is often necessary to include a higher number of boards to ensure that this *whole* sample is representative for the timber source and the species, range of sizes and quality of timber to be graded in production. Each country or standardised area included in the setting area, i.e. the combination of countries or standardized areas in which the same settings shall be applied, must be represented by a minimum of 100 boards. A standardised area consists of countries for which the same settings can be applied without any further justification. The standardised areas specified in EN 14081-2 (2018) are given in Table 8. Furthermore, the timber shall be sawfalling, i.e. the boards shall not be pre-graded, and the boards shall have the most demanding surface finish for the performance of the machine(s). Boards that include a defect that would be rejected by a visual override inspection, see EN 14081-1 (2016), shall not be included.

Table 8: Standardised areas defined in EN 14081-2 (2018).

Standardised area	Countries included
Alp area	Liechtenstein[1], Slovenia, Switzerland, Austria
Balkan area	Montenegro[1], Macedonia, Albania, Bosnia-Herzegovina, Croatia, Serbia, Kosovo
Baltic area	Estonia, Latvia, Lithuania
Benelux area	Luxembourg, Belgium, Netherlands
Black Sea area	Moldova, Romania
French area	Andorra[1], France

[1)] These countries alone cannot be considered representative for the standardized area

As regards dimensions of boards, the whole sample shall include at least 40 boards within the 10 % range of the smallest width, and at least 40 boards within 10 % range of the largest width, intended to be graded in production. A corresponding requirement is applied for the smallest and larges thicknesses.

The whole sample shall also include a minimum of 40 boards with the smallest cross-sectional area. Furthermore, the smallest cross-sectional area intended to be graded in production shall not be extrapolated more than 10 % from the smallest cross-section area of boards included in the whole sample.

3.3.2.3 Collection of data from the grading machine

All boards included in the whole sample shall pass through the grading machine or combination of machines while the data that give basis for the IP or the IPs are recorded for each board. The boards shall pass through the machine(s) at its/their critical feed speed, i.e. the speed within the intended operational range at which the grading machine gives the least accurate data as basis for calculation of IP/IPs.

3.3.2.4 Destructive testing

All boards included in the whole sample shall be tested in accordance with EN 408 (2010) and EN 384 (2016) to determine each board's strength, MOE and density.

When settings shall be determined for the T-classes, the following board properties shall be tested for each board: tensile strength ($f_{t,0}$), see *Eqs. 12* and *14*, MOE parallel to the grain ($E_{t,0}$), see *Eq. 9*, and clear wood density ($\rho_{12\%}$), see *Eq. 3*. The clear wood density shall, in accordance with EN 408 (2010), be determined using a specimen free of knots and resin pockets cut as near as possible to the fracture zone.

When settings shall be determined for the C and D-classes, the following board properties shall be tested for each board: bending strength (f_m), see *Eqs. 13* and *14*, MOE parallel to the grain ($E_{m,0}$), see *Eqs. 10* or *11*, and clear wood density determined as described in the previous paragraph. A compilation of applied board properties when determining settings for C, D and T-classes are given in Table 9.

Table 9: Board properties that shall be tested in accordance with EN 408 (2010) and EN 384 (2016) when settings are determined for T-classes or C- and D-classes.

Grades / Board property	C- and D-classes	T-classes
Strength	f_m	$f_{t,0}$
MOE	$E_{m,0}$	$E_{t,0}$
Density	$\rho_{12\%}$	$\rho_{12\%}$

3.3.2.5 Derivation of settings

The procedure of deriving settings for a new machine type is no longer normative, which it was until 2018. However, in EN 14081-2 (2018), Annex B,

an informative method based on linear regression is given, which can be applied when deriving settings. This method is called the Prediction limit method.

Settings for an IP/IPs shall be determined such that the minimum requirements of characteristic values of the GDP are fulfilled when all boards having IPs exceeding the settings are assigned to the graded class. For the T-classes, settings are determined such that the boards assigned to a grade have a 5-percentile characteristic tensile strength parallel to the board direction ($f_{t,0,k}$), a 5-percentile characteristic density (ρ_k) and a mean characteristic MOE parallel to grain ($E_{t,0,mean}$) that exceed the minimum requirements of the graded T-class. Similarly, structural timber, which is graded to C- and D-classes, must have a 5-percentile characteristic bending strength ($f_{m,k}$), a 5-percentile characteristic density (ρ_k) and a mean characteristic MOE parallel to grain ($E_{m,0,mean}$) that exceed the minimum requirements of the graded class. The characteristic values of the sample of boards assigned to a grade are determined in accordance with EN 14358 (2016) and EN 384 (2016).

The minimum requirements of 5-percentile characteristic strength, 5-percentile characteristic density and mean characteristic MOE parallel to grain of each strength class are given in EN 338 (2016). A few of the T- and C-classes defined in this standard are given in Tables 5 – 6, respectively. In these tables, the minimum requirements of 5-percentile characteristic strength, 5-percentile characteristic density and mean characteristic MOE are bolded.

Settings must be determined for each strength class and for each combination of strength classes intended to be graded in production. When settings are determined there shall be at least 20 boards assigned to each grade, and a minimum of 5 boards or 0.5 % of the total set of boards, whichever is higher, must be rejected.

3.3.2.6 Verification of settings

The settings determined as described in *Section 3.3.2.5 Derivation of settings* shall be verified in accordance with EN 14081-2 (2018). This verification of settings is carried out using the *whole sample* and so-called *verification samples* that are drawn from the whole sample. In total, there must be at least four verification samples. For each country or standardised area there shall be at least one verification sample only including boards from that country or standardised area. Verification of settings for a new machine type is carried out by checking that certain minimum requirements for both the whole sample and for the verification samples are fulfilled. The verification can be summarised as follows:

- The 5-percentile characteristic strength, 5-percentile characteristic density and the mean characteristic MOE of assigned boards from the whole sample to a grade must be equal to/or larger than their corresponding minimum requirements given in EN 338 (2016).

- The 5-percentile characteristic strength of assigned boards from each verification sample must be equal to/or larger than the minimum requirements of 5-percentile characteristic strength given in EN 338 (2016) multiplied by a factor of 0.9.

- The 5-percentile characteristic density of assigned boards from each verification sample must be equal to/or larger than the minimum requirements of 5-percentile characteristic density given in EN 338 (2016) multiplied by a factor of 0.9.

- The mean characteristic MOE of assigned boards from each verification sample must be equal to/or larger than the minimum requirements of mean characteristic MOE given in EN 338 (2016) multiplied by a factor of 0.95.

In addition, certain cost matrices shall be established and approved, see EN 14081-2 (2018), Annex C. Furthermore, a so-called repeatability test of the machine and applied IPs shall be performed using at least 100 boards, see EN 14081-2 (2018), clause 7.1.

The description given herein regarding derivation and verification of settings is intended to give an overview of the procedure for determination of settings of IP/IPs to be applied for a new machine type. However, it does not cover all the details. For the complete description, see EN 14081-2 (2018).

4. Scanning of wood

4.1 Automatic inspection of wood

Quality assessment of wood is important in many areas of the woodworking industry. For example, so-called *appearance grading* is based on quality assessment of the longitudinal surfaces of boards. In such grading each board is sorted into a certain G-grade on the basis of several characteristics visible at the surfaces such as, for example, knot types, size of knots, top ruptures, reaction wood, decay, insect attacks etcetera, but also on the basis of dimension errors and warp (EN 1611-1 1999). A purpose of these well-defined classes for appearance grading is to facilitate trade of timber.

Quality assessment of wood is also important in the manufacturing industries. For example, flooring, furniture and window manufacturers do not want to use wood that includes certain defects such as loose knots, i.e. knots that are not attached to its surrounding wood. If the end products include such knots, there is a risk that these knots eventually fall off and leave unwanted holes in the end products. Therefore, wood including certain defects must be identified and the parts of the wood including unwanted defects must be removed.

Automatic inspection by means of scanners is a common feature at different stages of the production chains in the woodworking industry. Already at the entrance at some sawmills, the quality of the wood within a log is evaluated using an X-ray Computed Tomography (CT) scanner. By means of a CT scanner, a log's local densities in three dimensions are obtained. Since knots have a density that differs from the density of clear wood, it is possible by means of measurements of a log's local densities to detect such defects before the log has been cut. Logs can thus be rotated and the sawing pattern determined such that the boards are cut in an optimized manner for their intended use. Figure 11 shows an example of measurement results obtained by means of a CT log scanner. Note that the entire local density variation within the log is known, but, in this figure a threshold value has been set such that only the parts of the log having a higher density than the set threshold are visible.

Automatic inspection of boards can be carried out by means of optical scanning and/or unidirectional X-ray scanning. Regarding the latter, as shown in *Section 2.2.2.1 Density*, such X-ray scanning results in a high-resolution two-dimensional density plot, and as mentioned in the previous paragraph, since knots have a density that differs from the density of clear wood, sections including such defects can thus be identified and, if necessary, removed by a saw later on in the production line. In an optical scanner, board surfaces are evaluated by means of photographs taken by colour cameras and/or multisensor cameras while simultaneously illuminating the surfaces by, for instance, led lighting, dot-lasers and line-lasers. The purpose of such scanners is to identify

defects visible on the boards' surfaces such as, for example, knots, decay, and cracks. An example of the set up of cameras and lasers in a commercial optical wood scanner is shown in Figure 12. In the exhibited setup, boards are fed through the scanner in their longitudinal direction while photographs of the surfaces and other measurement results are continuously evaluated using a computer to identify certain defects.

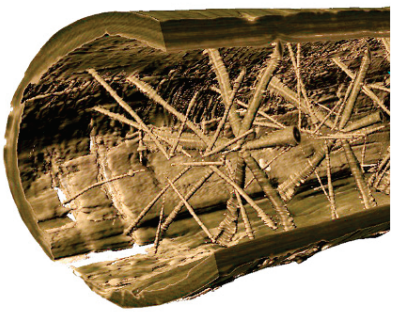

Figure 11: Result from a CT scan of a part of a log. Photo by courtesy of Microtec.

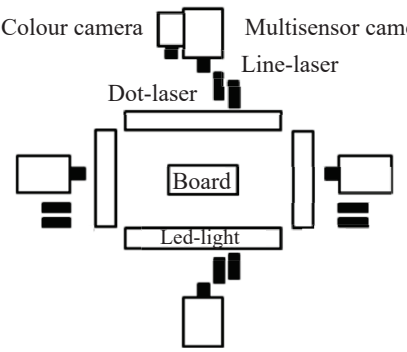

Figure 12: Set up of cameras and lasers in a commercial optical wood scanner.

4.2 Tracheid effect

Fibres in softwood spread concentrated light, such as laser light, better in the length direction of the fibres than in their transverse directions (Matthews & Beech 1976; Nyström 2003; Åstrand 1996). When a circular beam of concentrated light illuminates a softwood surface, a part of the light is directly reflected from the wood surface whereas another part penetrates the surface and scatter within the wood. The latter part is then, according to Soest et al. (1993), transmitted within the cell lumens and when it reaches the walls and ends of the

cells, a part of that light will be reflected back to the surface whereas another part will continue to scatter to adjacent cells. Since both the cells and corresponding lumens have an oblong shape, most of this light scattering will occur in the length direction of the fibres. At the wood surface, the reflected light will enter a shape that resembles an ellipse with its major axis oriented as a projection of the longitudinal fibre direction onto the surface. This projected fibre direction is also called the *in-plane fibre direction*. The light scattering that occurs within wood when it is illuminated by a circular beam of concentrated light is known as the tracheid effect. An example of this effect is shown in Figure 3.

The tracheid effect is applied in optical wood scanners as an application for detection of defects at wood surfaces, such as round knots. Since light conduction occurs mainly in the length direction of fibres, which at a surface of a round knot are directed perpendicular to the surface, round knot surfaces spread far less light than its surrounding clear wood. Generally, the shape of reflected light on the surface is almost circular when the surface of such a knot is illuminated.

4.2.1 In-plane fibre direction

The 3D direction of fibres can be defined by means of an in-plane angle and an out-of-plane angle, which is illustrated in Figure 13. In this figure, the vector $\mathbf{u}$ represents the direction, in 3D, of a single fibre. Let the *xy-plane* represent the wood surface, where the *y*-axis is in the longitudinal direction of the specimen (or board) and the *x*-axis is oriented in the board's transverse direction. The in-plane fibre direction is then defined by the vector $\mathbf{u}_{xy}$.

The major axis of the ellipse of the spread of light, which occurs when a wood surface is illuminated by a dot-laser, see Figure 3, is oriented in the same direction as the projection, onto the surface, of the length direction of the fibres, i.e. in the same direction as vector $\mathbf{u}_{xy}$. By means of the vector $\mathbf{u}_{xy}$ and the unit vector $\mathbf{v}_y$, the in-plane fibre direction can be determined in relation to the longitudinal direction of the specimen by the angle (α) between the two vectors, which is calculated as

$$\cos\alpha = \frac{\mathbf{u}_{xy} \cdot \mathbf{v}_y}{\left(\left|\mathbf{u}_{xy}\right|\left|\mathbf{v}_y\right|\right)}. \tag{24}$$

As mentioned earlier, illumination of a wood surface using high-intensity light, such as a beam of laser light, results in the scattering of light in several fibres close to the surface. For example, Nyström (2003) reported that the ellipse can have a length of 10 mm and a similar length is presented in the attached Paper III. Thus, since the spread of light occurs in several fibres, it must be realized that the fibre direction determined by means of the tracheid effect

represents an average direction of all fibres through which the light from a beam of high-intensity light is scattered. In the vicinity of knots, the length direction of the fibres deviate considerably from the length direction of fibres in clear wood and, generally, this transition zone is smaller than the size of the ellipse of scattered and reflected light that occurs on the illuminated surface. As a result, when illuminating such a transition zone between a knot and its surrounding clear wood, the shape of the scattered and reflected light on the surface might not be elliptic.

Most studies involving the tracheid effect have been carried out on softwood species, like for instance Norway spruce. However, the performance of the tracheid effect on hardwood species has also been investigated. The results of a recently published study carried out by Besseau et al. (2019), show successful application of the tracheid effect for the hardwood species oak (*Quercus petraea* and *Quercus robur L*) and Sweet chestnut (*Castanea*).

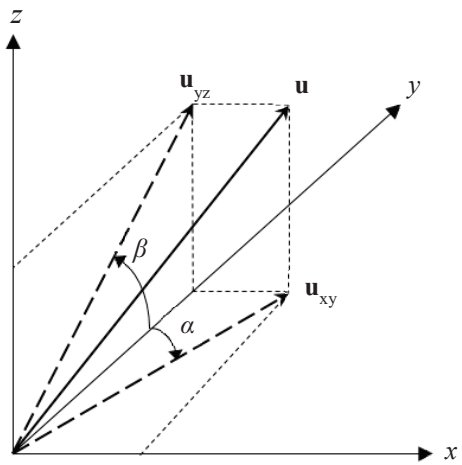

Figure 13: Illustration of a fibre's direction in 3D, represented by the vector **u**. *By means of the tracheid effect it is possible to determine the projection of* **u** *on the xy-plane (i.e.* $\mathbf{u}_{xy}$*).*

4.2.2 Out-of-plane fibre direction

In earlier investigations (Kandler et al. 2015; Olsson & Oscarsson 2014; Simonaho et al. 2004) it has been suggested that the absolute value of the out-of-plane angle (β) of fibres, see Figure 13, can be determined using a mapping between out-of-plane angle and the ratio between minor and major axes of the ellipse of the spread of light. The latter ratio will from here on be referred to as *shape factor ratio*.

Simonaho et al. (2004) obtained, on the basis of observations of shape factor ratios and out-of-plane angles of silver birch and Scots pine, the following relationship between the shape factor ratio and the out-of-plane angle:

$$\beta = \frac{1}{2}\cos^{-1}\left(\left(\frac{l_1 + l_2}{2} - r\right)\cdot\frac{2}{l_2 - l_1}\right) \tag{25}$$

where l_1 and l_2 are the shape factor ratios at 0˚ and 90˚ degrees, respectively, and r is the shape factor ratio of an observed elliptical laser dot on the surface. The values of l_1 and l_2 were not explicitly given in their paper, but, from one of the included figures, these can be interpreted as 0.21 and 0.91, respectively. Olsson and Oscarsson (2014) used another set of observations, from measurements carried out on Norway spruce, and obtained a best-fitted mathematical function in the same form as *Eq. 25* for their observations, but with another set of values of l_1 and l_2. These values were set to 0.54 and 0.82, respectively. In another investigation of Norway spruce carried out by Kandler et al. 2015 a third set of observations of shape factor ratios and out-plane angles was used, and they obtained the best-fitted mathematical function as

$$\beta = \sin^{-1}\left(\frac{r - l_1}{1 - l_1}\right) \tag{26}$$

with an l_1-value of 0.54. The three above-mentioned relationships identified between shape factor ratios out-of-plane angles are shown in Figure 14.

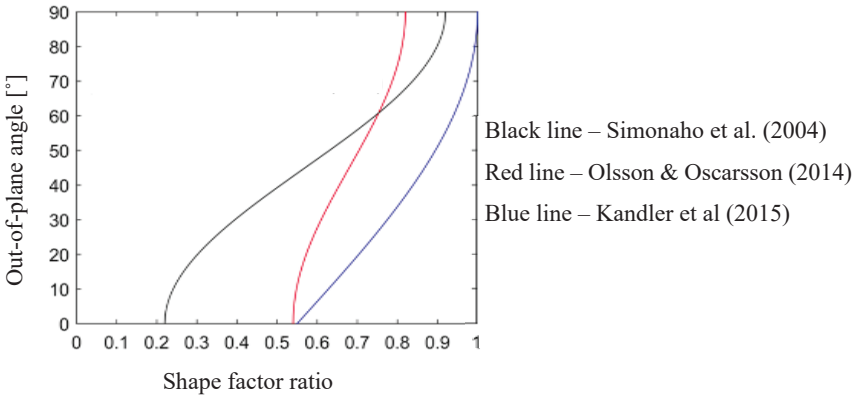

Figure 14: Fitted mathematical functions between shape factor ratios and out-of-plane angles from three different investigations. Simonaho et al. (2004) investigated silver birch and Scots pine whereas Olsson and Oscarsson (2014) and Kandler et al. (2015) investigated Norway spruce.

The black solid line in this figure shows the mathematical function obtained by Simonaho et al. (2004), whereas the red and blue lines show the function determined by Olsson & Oscarsson (2014) and Kandler et al. (2015), respectively. In this context it must be mentioned that only the absolute value of the out-of-plane angle is obtained by means of the suggested mappings, i.e. it is not possible to determine if β is positive or negative solely based on the shape factor ratio.

4.2.3 Grading based on knowledge of in-plane fibre direction

Local fibre directions on the longitudinal surfaces of boards can be determined in high-resolution by means of optical wood scanners utilizing the tracheid effect. As the boards are fed through such a wood scanner, a number of laser beams will illuminate the longitudinal board surfaces. By means of photographs taken of the spread of laser light on board surfaces, in-plane fibre directions for every illuminated point are determined. The in-plane fibre directions determined for the surface displayed in Figure 15a are shown in Figure 15b.

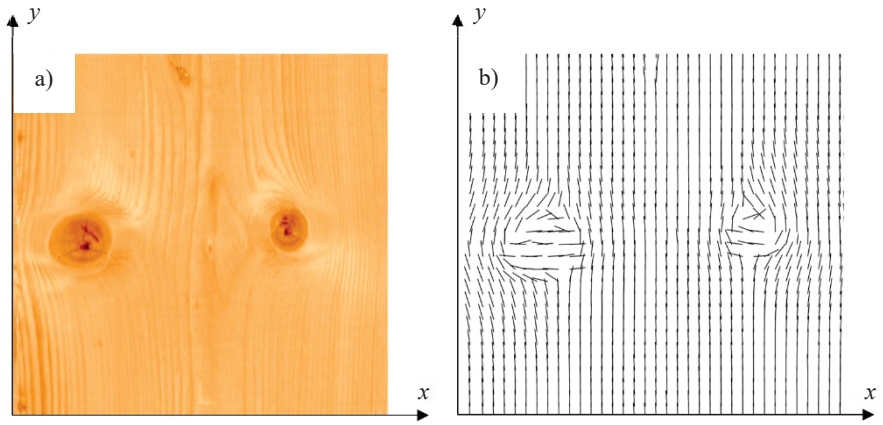

Figure 15: a) Surface of Norway spruce, and b) determined in-plane fibre directions for the surface exhibited in a).

Olsson et al. (2013) suggested a new strength grading method based on the tracheid effect for grading of structural timber. In 2015, a grading report for this method was approved by CEN/TC124/WG2/TG1 for grading of structural timber of Norway spruce (Olsson & Oscarsson 2017). The procedure to determine the IP applied for prediction of strength can be summarised as follows: firstly, by means of surface laser scanning and dynamic excitation, the in-plane fibre directions at the longitudinal surfaces and the axial resonance frequency, respectively, are determined. Secondly, by means of the observed in-plane fibre directions, board dimensions and the axial dynamic MOE, a bending stiffness profile in terms of a bending MOE-profile is calculated along

the longitudinal direction of the board, see Figure 16. The lowest value along this MOE-profile is then applied as IP to strength. The method is described in some detail in paper IV.

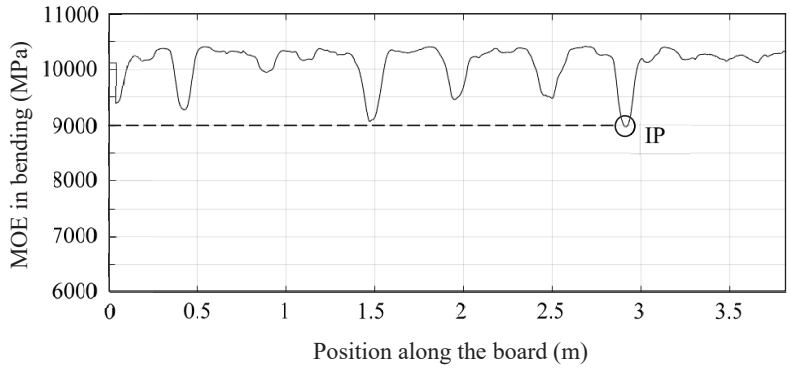

Figure 16: a) A bending MOE-profile of a board calculated on the basis of measured in-plane fibre direction and axial dynamic MOE. The lowest value along this profile is applied as an IP to strength.

Olsson and Oscarsson (2017) investigated a total number of 936 boards of Norway spruce, and single linear regression between the described IP and bending strength resulted in an r^2 of 0.69. For the same sample, the r^2 between axial dynamic MOE and bending strength was 0.53.

Olsson et al. (2018) used a similar IP for prediction of bending strength of Douglas fir and European oak. For Douglas fir, they obtained an r^2 of 0.62 between the suggested IP and bending strength. For the same sample, using the axial dynamic MOE as IP, an r^2 of 0.47 was obtained. For European oak, the IP based on fibre direction and axial dynamic MOE resulted in an r^2 of 0.59 to bending strength (c.f. with an r^2 of 0.22 when only axial dynamic MOE was applied as IP). The sample of European oak, however, only included boards with dimensions 22 × 100 mm. i.e. the presented r^2 values for European oak must be interpreted with caution.

The proposed grading models are based on assumptions regarding the fibre direction. Firstly, the out-of-plane angle is disregarded, i.e. it is set to zero for all observations. If the out-of-plane angle could be included in the model, it is possible that an even better grading model could be established. Secondly, the local in-plane fibre direction determined at the surface is assumed to be valid for a certain depth into the board, i.e. for a certain small volume, see Figure 17b. As can be seen in Figure 17b, no consideration is taken to direction of knots within the interior of the board. Additional information regarding the interior of the board could be used to model the fibre direction with the interior of a board more precisely, which in turn could enable more accurate grading. On this basis, Hu et al. (2018) suggested an alternative approach, taking location of pith and

implicitly orientation of knots into account, to model the fibre direction within the interior of the board, see Figure 17c. In this model the fibre direction within the interior of the board are determined by linear interpolation in radial direction between surfaces. Hu et al. (2018) evaluated the two models exhibited in Figures 17b − c by comparing the calculated MOE-profiles of two boards of Norway spruce with corresponding MOE-profiles calculated on the basis of strains determined using digital image correlation applied on boards subjected to four-point bending. The model taking location of pith into account, i.e. the one illustrated in Figure 17c, gave a more accurate calculation of local bending stiffness. Moreover, by combining this model of fibre directions with a finite element solid model, a very close resemblance between calculated and experimentally based bending stiffness profiles was obtained. However, as regards strength prediction, no significant improvement was achieved using the modelled displayed in c) compared to the one exhibited in b) (Hu 2018).

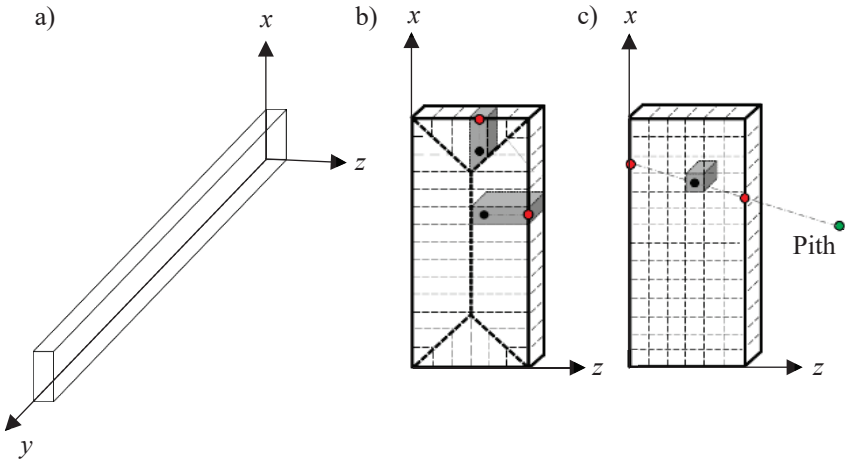

Figure 17: a) Illustration of applied coordinate system. b)−c) Models for representation of the fibre direction within the interior of the board. Figures by courtesy of Hu et al. (2018).

5. Research contribution

5.1 Paper I

The purpose of paper I was to define a scheme for how models of the 3D orientation of knots in boards can be established on the basis of tracheid effect data from high-speed laser scanning. Since the orientation of a knot is decisive for the orientation of fibres flowing around or integrating with the knot, the development of 3D knot models is regarded an important step towards modelling the entire 3D fibre structure within a board. The aims of paper I were

- to determine positions and areas of knot surfaces visible on different sides of a board,

- to identify knot surfaces belonging to the same physical knot and create a 3D model including all knots within the board, and

- to determine the location of the pith along the board on the basis of the orientation of the identified knots.

In the proposed algorithm, the 3D fibre directions at longitudinal surfaces of boards are determined by means of the in-plane and the out-of-plane fibre directions obtained by tracheid effect scanning. For each dot-laser illumination, the angle between the 3D fibre direction and the length direction of the board is calculated. If this angle exceeds a certain threshold value, the observation is determined to be part of a knot surface. Examples of knot surfaces identified by the algorithm are shown in Figure 18a. The red colour in this figure corresponds to a large angle between the 3D fibre direction and the length direction of the board, i.e. a knot surface, whereas the blue colour corresponds to a small angle between the 3D fibre direction and the length direction of the board.

A polar coordinate system is then defined using the location of the pith of the log at one of the end cross-sections, see Figure 18b. If the difference in centre positions of identified knot surfaces in the length direction of the boards, i.e. y-direction, and the angle $d\theta$, see Figures 18a − b, are below certain threshold values, knot surfaces are determined to be parts of the same knot. Each knot volume is then modelled as a convex hull, i.e. as the smallest convex volume that connects the different knot surfaces as shown in Figure 18a.

The algorithm developed for identification of knot surfaces, and the determination of knot volumes, proved to work well. A close examination of teen boards of Norway spruce showed that almost all knots with surface areas larger than 100 mm^2 were identified using the algorithm and also that knots having visible surfaces larger than 100 mm^2 were, with very few exceptions,

correctly associated with other surfaces of the same knot. Knot surfaces smaller than 20 mm^2, i.e. smaller than 5 mm in diameter, were often neglected by the algorithm but when identified at all, they were correctly connected to other identified knot surfaces that were parts of the same knot. In a few cases, poor planing resulted in rough surfaces mistakenly being identified as knots.

Knot volumes and the direction of the pith of the knots are in the suggested algorithm utilised for determination of the location of the pith of the log along the board. Using knot volumes including only round knot surfaces, the pith of each knot is approximated by a vector drawn through the centre of the two identified knot surfaces, see Figure 18c. The location of the pith of the log along the board is then approximated by the straight line that minimises the sum of squared smallest distances between this straight line (thicker black line in Figure 18c) and the lines representing the piths of the knots (red lines in Figure 18c). Results of such calculations were compared with the location of the pith at the board end sections, as they were indicated by the annual ring pattern, and the consistency of the results was satisfactory. However, determination of the position of the pith of the log, as it is done on the basis of the direction of knots in the algorithm, requires that the pith of the log is located outside the board's boundaries. Another limitation is that some knowledge of an approximate location of pith is required, already from the outset.

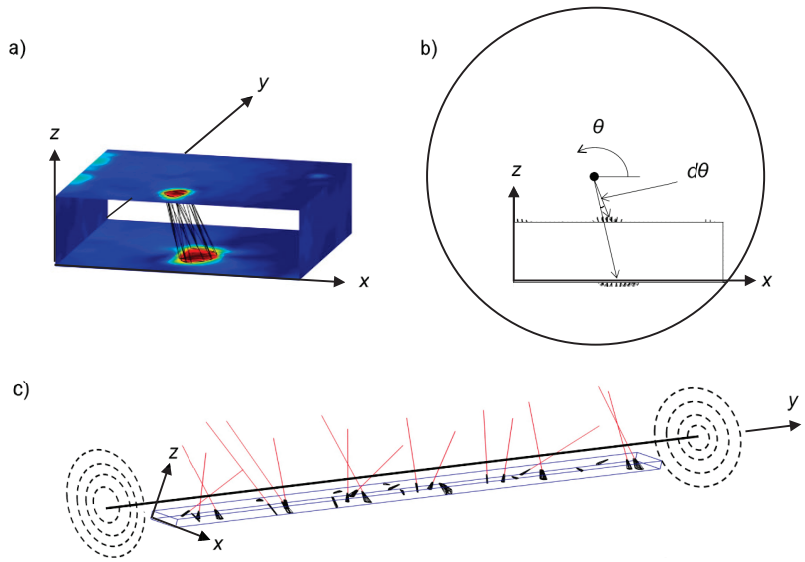

Figure 18: a) Three-dimensional view of identified knot surfaces, and knot volume modelled as a convex hull. b) Cross-section of a board encapsulated within the log from which it is sawn and a knot marked out on two surfaces and indicated with respect to position with polar coordinates. c) Contour lines of a 4.8 m long part of a board and all the knots identified within it, along with an indication (thick black line) of the position of the pith of the log.

A contribution of paper I is that it shows that surface laser scanning can be used to gain knowledge not only of the fibre orientation on scanned surfaces, in the plane of these surfaces, but also of the location, size and direction of knots in 3D. This is an important step towards accurate models of 3D fibre orientation of individual timber members, which should give basis for development of new or improved methods for accurate prediction of strength of structural timber.

5.2 Paper II

The purposes of paper II were to investigate the 3D fibre direction and the 3D growth layer orientation in the vicinity of a knot. The aims of the research were to

- develop a laboratory method for determination of 3D growth layer geometry,

- develop a laboratory method for determination of high-resolution 3D fibre orientation in the vicinity of knots, and

- determine the local longitudinal, radial and tangential material directions, at any position within an investigated wood specimen.

The study was carried out using a single specimen of Norway spruce containing a knot. The specimen was prepared such that it included the pith of the tree and a complete knot, with margins of wood on all sides of the knot. It was assumed that a plane of symmetry existed both through the entire specimen and through the knot. By splitting the specimen through this plane, i.e. through the pith of the knot and the pith of the tree, two new specimens with assumed identical but mirrored properties were achieved. On one of the new specimens, the longitudinal-radial plane was subsequently scanned whereas the longitudinal-tangential plane was scanned on the other. Then, by repeatedly planing off material on both specimens followed by scanning of the new surfaces that gradually appeared, 3D coordinate positions along different growth layers and 3D direction of fibres in a 3D grid were obtained. The growth layers were determined by tracing each investigated layer in images obtained by means of a flatbed scanner, and the 3D fibre orientation in the vicinity of the investigated knot was determined using the in-plane fibre directions obtained by means of dot-laser illuminations.

As regards the accuracy of the determined fibre directions in 3D, see Figure 19, it was shown that the angle between fibre direction and the normal direction of a growth layer surface was, when both directions were determined at the same position, in general very close to 90˚. Any discrepancy from a 90˚ angle would suggest an error since fibres must be oriented within the plane of a growth layer.

The obtained results of growth layers showed that a knot/branch causes a pronounced local effect, a swelling, on the geometry of the growth layer close to the knot, whereas the bulk of the growth layer forms a cylindrically shaped surface with its longitudinal direction close to parallel with the pith of the tree/log. This was well known from before. However, the quantitative data obtained using the proposed method give basis for calibration of parameters of included in mathematical models of growth layer geometry and fibre orientation close to knots on a millimeter scale.

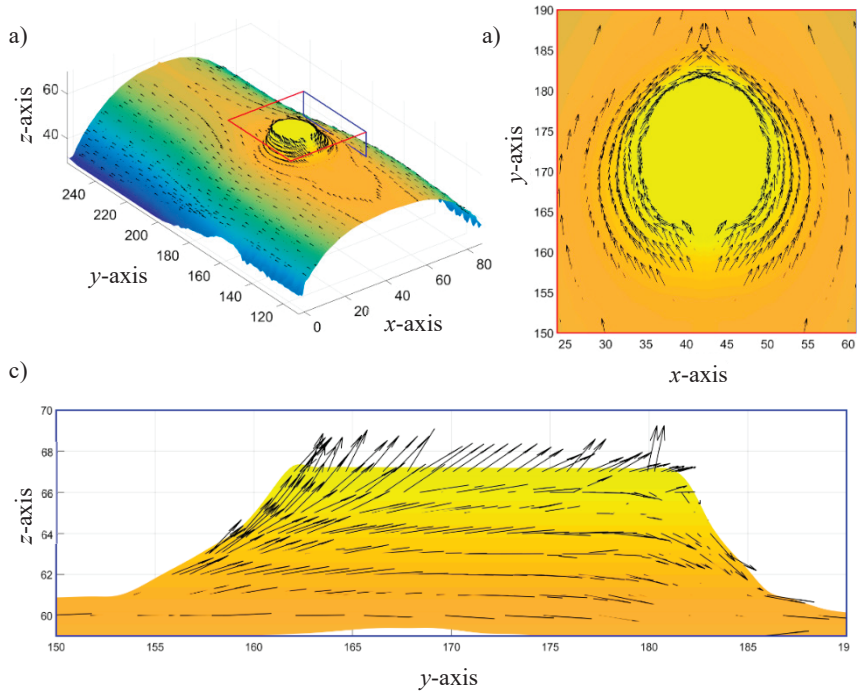

Figure 19: The 3D fibre directions for one of the investigated growth layers. The colours indicates the variation of z-coordinate of the shown growth layer whereas the arrows show the 3D local fibre direction. The figures displayed in a), b) and c) show a 3D view, an enlarged xy-view and an enlarged yz-view, respectively.

5.3 Paper III

The purpose of the research presented in paper III was to contribute to knowledge and development of non-destructive methods for determination of the 3D fibre direction of timber, especially in the surroundings of knots. The purpose can be divided into two particular aims, namely to

- investigate, for Norway spruce timber, the relationship between the shape of reflected light from a dot laser, i.e. of a greyscale image of reflected light, of an illuminated wood surface and the out-of-plane angle of the fibres at the surface, and

- validate a model, proposed by Foley (2003), for the fibre direction in the vicinity of knots in the radial-longitudinal plane and to discuss the potential applicability and limitations of this model for engineering purposes.

The study was carried out using the data obtained from the specimen described in *Section 5.2 Paper II*, and the same assumption, that a plane of symmetry existed through the investigated specimen and the knot, was applied. As mentioned previously, after splitting the specimen along this plane of symmetry, dot laser illuminations were carried out on orthogonal planes, i.e. on longitudinal-radial planes and on longitudinal-tangential planes.

The sampled data was used to investigate the relationship between shape factor ratios (obtained from surfaces of the one half of the specimen) and out-of-plane angles (determined on the, so to speak, mirrored positions on the other half of the specimen), and it was found that the relationship between these two entities was rather weak, see Figure 20. It was also observed that the size of the ellipse of reflected laser light, as well as the shape factor ratio, differ between earlywood and latewood, which may be one of the explanations for the weak correlation. The size of the reflected laser light on clear wood was as large as approximately 10 × 5 mm in the fibre direction and in the transverse direction of the fibres, respectively. Thus, when illuminating the close surrounding of a knot, fibres both within and outside the knot reflected light, and on such surfaces the reflected light did not resemble the shape of an ellipse at all.

The sampled data was also used to compare the mathematical equation given by Foley (2003) for the fibre direction in the vicinity of a live knot region in the radial-longitudinal plane. The correspondence between fibre direction calculated using the model and fibre direction determined on the basis of the tracheid effect was very good. Fibre directions calculated using the mathematical model proposed by Foley (2003) were, however, sensitive to the geometry of the knot. Even comparatively small errors of the assumed knot geometry led to substantial inaccuracy of calculated fibre directions.

In conclusion, tracheid effect scanning gives reliable data of in-plane fibre directions on timber surfaces but not, according to our results, of out-plane-angles. The shape factor ratio helps, however, to indicate knot surfaces. The model presented by Foley (2003) gives accurate information of 3D fibre directions in the surroundings of knots, but only if the geometry of the knots that governs the fibre directions is known in detail.

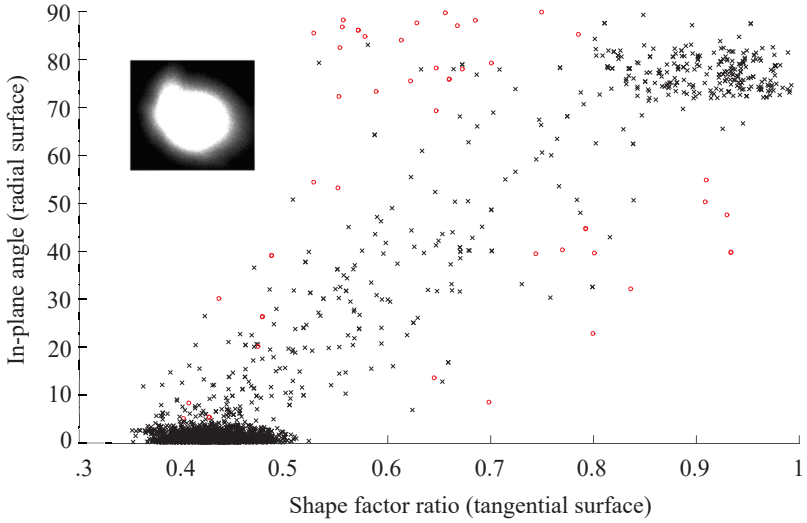

Figure 20: Scatter plot of observed in-plane angles and corresponding shape factor ratios of about 2000 observations. The in-plane angles measured on radial wood surfaces correspond to the out-of-plane angles for shape factor ratios measured on tangential wood surfaces. The infolded image shows an example of the irregular shape of the spread of light of an observation at the boundary of the knot. The points marked by red circles represent observations where the spread of light takes such irregular shapes.

5.4 Paper IV

The work presented in paper IV was part of a full-scale investigation with the purpose of achieving a formal approval of grading sawn timber to T-classes using a grading method very similar to the one suggested in Olsson et al. (2013). The results of the investigation are presented in two papers and paper IV is the first of these. The aims of paper IV were as follows:

- To define and evaluate IPs based on observed in-plane fibre directions on longitudinal board surfaces and on axial dynamic MOE. This includes evaluation of statistical relationships between IPs and GDPs used for grading of sawn timber into T-classes.

- To evaluate the significance of the surface finish (sawn or planed surfaces, respectively) when performing surface laser scanning of boards, i.e. to evaluate how IPs and grading accuracy are affected when based on data from surface laser scanning of sawn rather than of planed board surfaces.

The results presented in paper IV are based on investigations of a total number of 967 boards of Norway spruce originating from Finland, Norway and Sweden. All boards had sawn surface finish at the time of the sampling. The material was gathered in accordance with the sampling requirements given in EN 14081-2 (2010). Since then this standard has been replaced by the current version EN 14081-2 (2018) which means that the material was not sampled following the requirements described in *Section 3.3.2.2 Requirements of sampling* but according to the now obsolete version of the standard. A detailed description of the sampling requirements given in EN 14081-2 (2010) is given in Paper IV.

In the paper, two new IPs are presented, which were derived by means of multiple linear regression based on results from both non-destructive and destructive testing. These IPs are defined as

$$IP_{\mathrm{E,a}}(E_{\mathrm{a,90,nom}}, E_{\mathrm{dyn,12\%}}) = k_0 + k_1 \cdot E_{\mathrm{a,90,nom}} + k_2 \cdot E_{\mathrm{dyn,12\%}} \tag{27}$$

and

$$IP_{\mathrm{E,b}}(E_{\mathrm{b,90,nom}}, E_{\mathrm{dyn,12\%}}) = k_3 + k_4 \cdot E_{\mathrm{b,90,nom}} + k_5 \cdot E_{\mathrm{dyn,12\%}} \tag{28}$$

where k_0, k_1, k_2 and k_3, k_4, k_5 are the regression coefficients between the predictor variables $E_{\mathrm{dyn,12\%}}$ and $E_{\mathrm{a,90,nom}}$ or $E_{\mathrm{b,90,nom}}$ and the dependent variable $f_{\mathrm{t,0,h}}$, see *Eq. 12,* obtained by the least square method. The index h of $f_{\mathrm{t,0,h}}$ is used to mark that the determined tensile strength of each board with a width smaller than 150 mm has been divided by the size factor k_{h}, see *Eq. 14*. The predictor variables $E_{\mathrm{a,90,nom}}$ and $E_{\mathrm{b,90,nom}}$ are local axial and local bending MOEs, respectively, calculated on the basis of measured in-plane fibre direction at the board's longitudinal surfaces, whereas the predictor variable $E_{\mathrm{dyn,12\%}}$ is the dynamic MOE, see *Eq. 2*, adjusted to an MC of 12 %. A detailed description and definitions of the properties $E_{\mathrm{a,90,nom}}$, $E_{\mathrm{b,90,nom}}$ and $E_{\mathrm{dyn,12\%}}$ are given in paper IV.

All boards were scanned to determine local in-plane fibre directions, first when the boards had a sawn surface finish and then again after planing. For most of the boards, the in-plane fibre directions obtained before and after planing, were almost identical. For some boards, however, surface laser scans carried out before planing on rough sawn surfaces indicated irregular fibre directions even on knot-free surfaces.

The IPs introduced in this paper, see *Eqs. 27 − 28*, resulted in higher coefficients of determination and lower SEEs to $f_{\mathrm{t,0,h}}$ than what other IPs such as $E_{\mathrm{dyn,12\%}}$ did. For example, linear regression between $f_{\mathrm{t,0,h}}$ and $IP_{\mathrm{E,b}}$ calculated by means of measurement results obtained before and after planing resulted in coefficients of determination of 0.65 and 0.66, respectively, see Figures 21a − b,

whereas linear regression between $f_{t,0,h}$ and $E_{dyn,12\%}$ resulted in coefficients of determination of 0.46.

As can be seen in Figures 21a − b, both scatter plots for $f_{t,0,h}$ and $IP_{E,b}$, before planing, see Figure 21a, and after planing, see Figure 21b, have a curvature. Using non-linear regression between $f_{t,0,h}$ and $IP_{E,b}$ resulted in coefficients of determinations as high as 0.68 when $IP_{E,b}$ was determined before planing and 0.70 when it was determined after planing.

A comparison of the results obtained in paper IV with the results presented in Hanhijärvi and Ranta-Maunus (2008), see Table 1, imply that the performance of both $IP_{E,a}$ and $IP_{E,b}$, as regards prediction of a board's tensile strength, would surpass the most accurate IPs used in grading machines today.

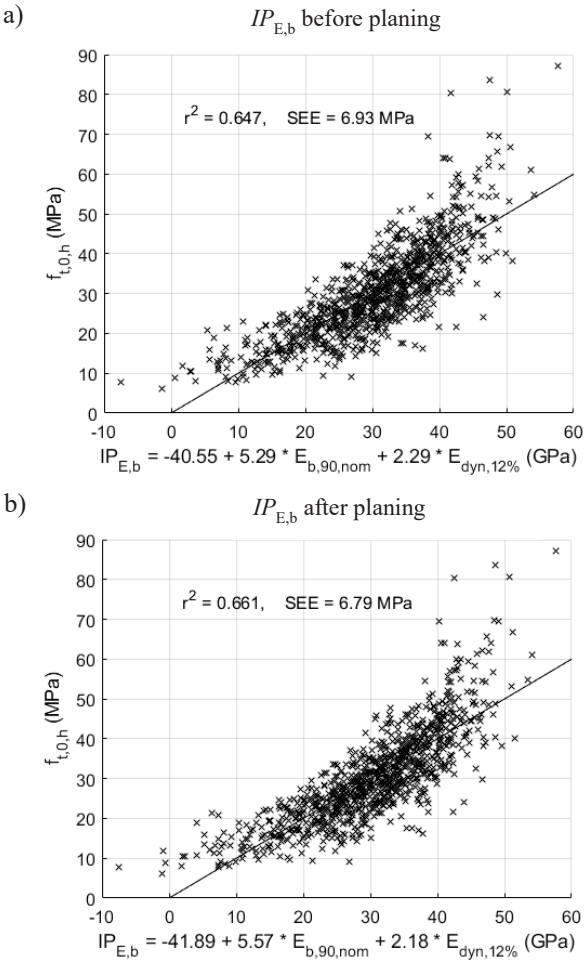

Figure 21: a)−b) Scatter plots between $IP_{E,b}$ and $f_{t,0,h}$.

5.5 Paper V

Paper V is the second and closing part in the series of two papers on prediction of GDPs and procedures for grading sawn timber into T-classes, based on the same material. The aims of paper V were to

- present two different, applicable procedures for determination of settings for grading methods based on IPs reflecting local board properties,

- determine settings for T-classes using $IP_{E,b}$ for strength, $E_{dyn,12\%}$ for MOE and board density at 12 % MC ($\rho_{s,12\%}$) for density and show how the yield in different strength classes depend on the procedure used for determination of settings, and

- discuss implications of the results on machine strength grading standards.

In *Section 2.2.2.3 Strength* it is described how the tensile strength of a board is determined in accordance with EN 384 (2016) and EN 408 (2010). As a background for paper V, it should be noted, in particular, that the tensile strength shall be determined by destructively testing a minimum length of 9h and that this destructively tested length shall include the anticipated weakest cross-section. It is also permitted according to EN 384 (2016) clause 5.2, to test a board's second anticipated weakest cross-section, if the anticipated weakest cross-section is too close to one of the boards ends. The weakest (or second weakest) cross-section can be determined by manual visual examination of the board's surfaces but this is only an estimation of a human and it is uncertain if the anticipated weakest testable cross-section actually is the weakest one. If the actually weakest cross-section of a board is not positioned within the tested length ($\geq$ 9h), when determining the board's strength, the determined strength is higher than what it would have been if the weakest cross-section had been included in the tested length.

In the paper a distinction is made between IPs that are based on global properties alone (global IP) and IPs that are based also on local properties (local IP). An example of a global IP is the axial dynamic MOE, see *Eq. 2*, which is calculated on the basis of the mass, the length and a resonance frequency of a board. An IP based on a global board property does not allow for any lengthwise resolution. A local board property, on the other hand, is associated with a local cross-section of the board. When determining settings for a new machine type, an IP representing a local board property can be defined as either the lowest local property along the entire length of the board or as the lowest local property

value along the part of the board actually tested, i.e. along the part of the board over which strength is evaluated. An illustration of this is shown in Figures 22a − b.

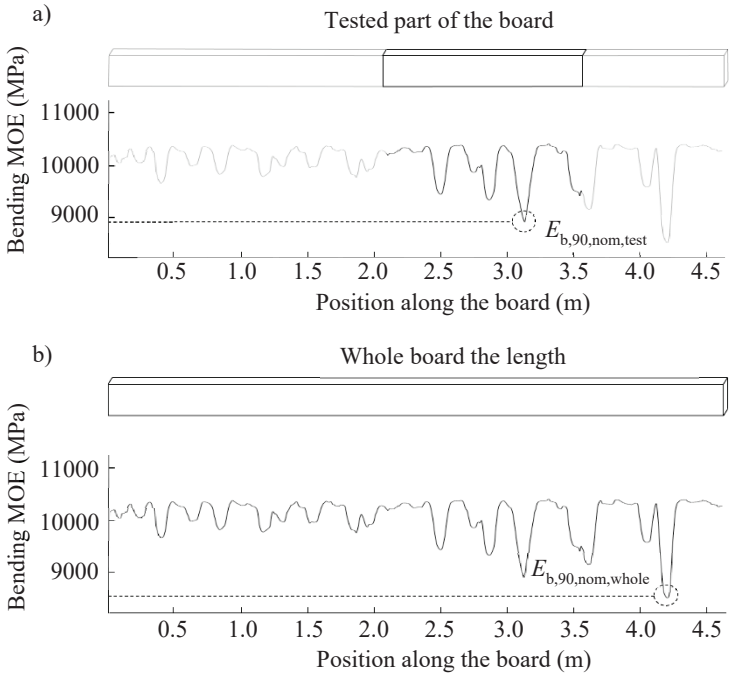

Figure 22: a) Lowest local property along the part of the board actually tested ($E_{b,90.nom,test}$), and b) lowest local property along the entire length of the board ($E_{b,90.nom,whole}$).

In paper V, two alternative procedures (Model 1 and Model 2) for determination of settings and calculation of yield for IPs reflecting a local board property are presented. In Model 1, settings are determined for $IP_{E,b}$ derived on the basis of $E_{b,90.nom,test}$, whereas in Model 2 settings are determined for $IP_{E,b}$ derived on the basis of $E_{b,90.nom,whole}$, see Figure 22 for definitions of $E_{b,90.nom,test}$ and $E_{b,90.nom,whole}$, respectively. For both models the actual grading was performed using $E_{b,90.nom,whole}$.

Model 2 resulted in a higher yield compared to Model 1 at the same time as the IP applied in Model 1 for prediction of the strength resulted in higher r^2 and lower *SEE* than what the IP applied in Model 2 did. The explanation for these, seemingly contradictory results, is based on the fact that the actually weakest cross section along a board was not always tested, which means that the actual strength of many boards, i.e. the strength of the very weakest cross section, is lower than the strength determined by the tensile test. Using Model 1, this condition is automatically and appropriately taken into account. Using Model

2, however, the yield in strength classes become too high. Grading on the basis of a global IP, such as dynamic MOE, is, in principle, comparable with application of Model 2.

It is shown in paper V that to guarantee appropriate grading, and in the end appropriate safety levels of timber structures, there is a need for further development of grading standards. Presently there is risk that the minimum requirement of 5-percentile characteristic strength given in EN 338 (2016) for a graded class are not fulfilled for timber graded in the daily production.

5.6 Paper VI

Finger joints in structural timber and glulam lamellae are often used to enable production of long timber boards or to allow for reconnection of parts of a board after removal of weak sections. In accordance with EN 15497 (2014), there shall be no knots or pronounced fibre disturbance within the joint itself. Outside the joint, a minimum distance of three times the knot diameter is required. The latter can be reduced to 1.5 times the knot diameter, i.e. an alternative criterion can be used, if an appropriate automated system guarantees that in the range of the finger joint the fibre direction is parallel to the longitudinal direction of the board. The aims of paper VI were to

- develop a procedure for accurate identification of knots on Norway spruce timber on the basis of surface scanning,

- make reasonable interpretations of the requirements of EN 15497 (2014) regarding unacceptable fibre deviations within finger joints of structural timber, and

- calculate the yield of different production cases of finger jointed structural timber, applying the alternative criteria for where finger joints are allowed

The study presented in paper VI was based on a sample including 897 boards of Norway spruce of dimension 45 × 145 mm. Even if the results are only valid for structural timber, they give a relevant indication also for glulam laminations.

It is shown in paper VI that accurate and robust detection of knots on wood surfaces can be done on the basis of knowledge of fibre direction on the four longitudinal surfaces obtained by surface laser scanning in combination with photographs of the surfaces. Both information from the laser scanning and the photographs can be obtained in high speed using an optical scanner.

As regards the interpretation of the requirement in EN 15497 (2014), i.e. that no pronounced fibre disturbance is allowed within finger joints, the following was considered: first, at what fibre angle tensile strength is substantially reduced

(compared to the strength of straight fibres) and second, that inclined fibres may occur in the timber independent of knots. Regarding tensile strength, and by application of the Hankinson formula (Hankinson 1921), a fibre angle of 8˚ means that the tensile strength is reduced by about 50%. Fibre angles smaller than 6 – 8˚, on the other hand, are sometimes caused by one or several of the following causes; spiral grain, skew sawing, taper and lack of accuracy of the detection of fibre orientation. Therefore, the smallest fibre angle considered herein as criteria for pronounced fibre disturbance was 8˚.

Figure 23a shows a calculated bending MOE profile of one board. The red lines in this figure indicate sections where a calculated bending MOE is lower than what would be required for strength class C35 (Olsson & Oscarsson 2017). In Figure 23b, photographs of four sides of the board are exhibited. The coloured horizontal lines in this figure indicate longitudinal sections that would pass for class C35 (green lines), sections that would not pass as C35 (red lines), sections that contain pronounced fibre disturbance according to a criteria defined on the basis of a fibre disturbance of 8˚ (black lines), sections with a knot present within a distance in longitudinal direction shorter than 1.5 times the knot diameter (blue lines) and sections with a knot present within a distance shorter than 3 times the knot diameter (purple lines). Figure 23c shows enlarged images of a 600 mm long part of the board. The vertically drawn purple arrows indicate where the board would be cut if the criterion of three times the knot diameter was applied to remove the weak section marked by the red field, i.e. the wood between the two purple arrows would then have to be discarded. The black arrows indicate where the board would be cut if the criterion of 1.5 times the knot diameter in combination with a criterion defined on the basis of fibre disturbance of 8˚ was applied instead. In the case illustrated in Figure 23c there is a short gap in the horizontally drawn purple line between the two purple arrows but since this gap is shorter than 30 mm, which is the assumed length of a finger joint, a finger joint cannot be placed there.

Based on the assumptions described in paper VI when using finger joints simply to produce timber of long lengths, the percentage of wasted material would decrease, according to simulations, from about 7.4 % to about 4.0 %, when using a combined criterion based on the fibre disturbance and the requirement of a margin of 1.5 times the knot diameter, rather than the simpler criterion of three times the knot diameter. Similarly, for a case where timber of long lengths with a quality corresponding to C35 is produced (weak sections removed) the wasted material would decrease from 28.1 % to 21.7 %.

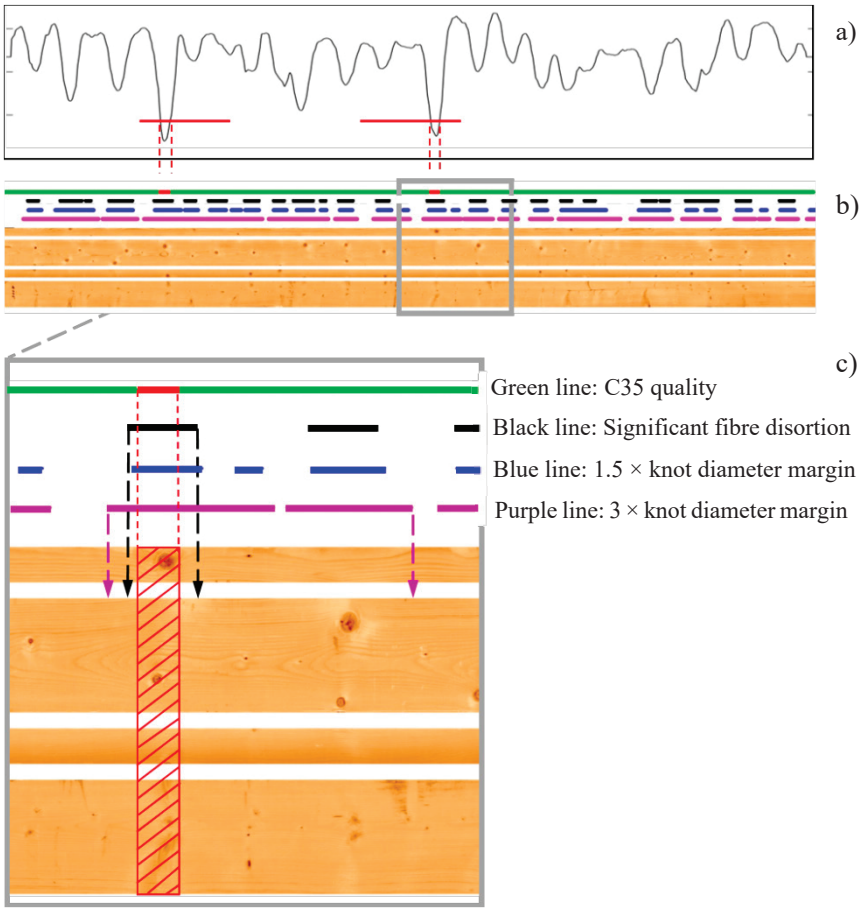

Figure 23: a) Calculated bending MOE profile, b) photographs of the four sides of the board, and c) enlarged photographs of a part of the board displayed in b). In b) and c) sections along the board that could pass for C35 quality are marked with a green line, sections where the board could be cut, and reconnected using finger joints, are marked with black, blue and purple lines, each colour representing a defined criterion.

6. Conclusions

The overall intention of this thesis work was to contribute to better utilisation of sawn timber and of lamellae for engineered products in construction. Today, much of the structural potential of timber is unused and a more efficient utilisation of sawn timber, which is made possible through more accurate grading of the material with respect to engineering properties, would make timber a more competitive load bearing material compared to concrete and steel. Development of accurate machine strength grading methods requires a profound understanding and accurate interpretation of the comprehensive data that is nowadays obtained using scanners, appropriate mechanical and material models by which such data is utilized, and thorough evaluation of the IPs to be used for grading.

The most important conclusions of the work presented in this thesis can be summarised as follows:

- Three-dimensional models of timber boards, including size, position and orientation of knots as well as location of pith along the boards, can be established on the basis of optical scanning and utilization of the tracheid effect.

- As regards the tracheid effect, application of the so-called shape factor ratio, i.e. the relationship between length and width of a spot of light from a concentrated source observed on the wood surface, resulted in a rather poor prediction of the out-of-plane angle of wood fibres. Still, the shape of the spread of light that occur when illuminating a surface with dot-lasers is useful for identification of knot areas at surfaces.

- An accurate IP for prediction of tensile strength can be obtained on the basis of local stiffness expressed in terms of an MOE, calculated on the basis of determined fibre directions at surfaces, in combination with axial dynamic MOE. For a sample of more than 900 boards, a proposed IP resulted in an r^2 as high as 0.66 (0.70 using nonlinear regression) which is considerably higher than what was obtained using axial dynamic MOE as IP to strength. For the same sample this gave an r^2 of 0.45.

- Application of the IP based on data from measurements of fibre direction and dynamic MOE, resulted in high yield in T-classes, which are used for glulam lamellae. For instance, the yield in the

grade T22 increased from 41 % to 52 % using the proposed IP, rather than axial dynamic MOE, for prediction of tensile strength.

- Finger joints in sawn timber must not contain knots or fibres that deviate significantly from the longitudinal direction of the board. By considering the fibre orientation observed on surfaces, rather than measures of knots alone, the waste of material in production of finger-jointed sawn timber can, for some production cases, be reduced by almost 50 %.

- When the tensile strength of a board is determined only a part of the board is actually tested. Thus, there may be other sections along the board that are actually weaker. If this is not properly taken into account in the grading procedure, there is a considerable risk that graded timber do not fulfill the requirements of the design values of the strength classes. When using IPs for prediction of strength that represents properties of local sections along boards the mentioned effect is normally taken into account. However, when using global IPs, such as axial dynamic MOE, it is not. In order to guarantee appropriate grading, the standard should be further developed to make sure that this effect is always taken into account.

7. Future work

More advance models of timber will lead to more accurate methods for strength grading, only if accurate data of local material properties and fibre directions are available and utilized. Therefore, the interface between extracting data from production-speed measurements and development of mechanical and material models should be in focus also in future research.

As shown and discussed in paper V, today's strength grading regulations make no distinction between IPs based on a local board property and IPs based on a global property when settings are determined. One important finding in this thesis work is that the determined settings for IPs representing a global board property, such as axial dynamic MOE, might result in the fact that the requirements of characteristic values, especially the 5-percentile characteristic strength, are not fulfilled for timber graded in industry. In the work presented in paper V, it is shown that this issue exists and needs to be considered. The influence of using a global board property when grading timber, thus, needs to be evaluated further and the grading regulations revised accordingly such that it is guaranteed that the requirements of characteristic values of boards graded by such IPs are fulfilled.

It has been shown in this thesis that very good material utilisation of glulam lamellae can be obtained by using a grading method based on surface laser scanning and dynamic excitation. A similar improvement is obtained for structural timber (Olsson & Oscarsson 2017). Another engineered wood product that is nowadays frequently used for construction is cross-laminated timber (CLT). CLT is normally produced using laminations graded as structural timber, i.e. into C- and D- classes, which are defined on the basis of edgewise bending strength. However, the laminations in the CLT elements are, in general, not loaded in bending. Also, the system effect is larger and different in CLT compared to for example glulam. Thus, for CLT lamella there may be more effective grade determining properties than the 5-percentile characteristic strength, which is decisive for the yield in C- and D-classes (bending strength) and T-classes (tensile strength), to use in definitions of strength classes. The author of this thesis, together with other researchers at Linnaeus University, intends to investigate possibilities for more effective grading of CLT lamellae in the future, both with respect to grading accuracy and to suitable grade determining properties.

8. References

ALSC (American Lumber Standard Committee, Incorporated) (2020). *List of approved machines*. http://www.alsc.org/greenbook%20collection/Grading_Machines.pdf. (Accessed 18 Feb 2020).

Bacher, M. (2008). *Comparison of different machine strength grading principles.* In: Proceedings of 2nd Conference of COST Action E53 – Quality control for wood and wood products, Delft, the Netherlands, October 29 – 30.

Besseau, B., Pot, G., Collet, R. & Viguier, J. (2019). *Measurement of fiber orientation by laser light scattering on dry and rough sawn green hardwood.* In: Proceedings of 21th International Non-destructive Testing and Evaluation of Wood Symposium, Freiburg, Germany, September 24 – 27.

Bohannan, B. (1966). *Effect of size on bending strength of wood members.* US Forest Service, Research paper FPL 56, Forest Products Laboratory, Madison, Wisconsin.

Bonakdar, F., Dodoo, A. & Gustavsson, L. (2014). *Cost-optimum analysis of building fabric renovation in a Swedish multi-storey residential building.* Energy and Buildings, 84: 662 – 673.

Brändström, J. (2001). *Micro- and ultrastructural aspects of Norway spruce tracheids: a review*. IAWA Journal, 22(4): 333 – 353.

Brändström, J., Bardage, S. L., Daniel, G. & Nilsson, T. (2003). *The structural organisation of the S1 cell wall layer of Norway spruce tracheids.* IAWA Journal, 24(1): 27 – 40.

Casselbrant, S., Kristensen, K., Müller, M., Raknes, E., Sipi, M. & Svensson, B. (2000). *Nordiskt kvalitetsspråk för träbranschen – Barrträd*. Swedish Institute for Wood Technology Research (Trätek), Report No. 9912058. (In Swedish).

Côté, W. A., Day, A. C., Kutscha, N. P. & Timell, T. E. (1967). *Studies on compression wood. V. Nature of the compression wood formed in the early springwood of conifers.* Holzforschung – International Journal of the Biology, Chemistry, Physics and Technology of Wood, 21(6): 180 – 186.

Dinwoodie, J. M. (2000). *Timber: Its nature and behaviour.* Second edition, E & FN Spon, London, UK.

Dodoo, A. (2019). *Lifecycle impacts of structural frame materials for multi-storey building systems*. Journal of Sustainable Architecture and Civil Engineering, 1(24): 17 – 28.

EN 338 (2016). *Structural timber – Strength classes*. European Committee for Standardization.

EN 384 (2016). *Structural timber – Determination of characteristics values of mechanical properties and density*. European Committee for Standardization.

EN 408 (2010) + A1 (2012). *Timber structures – Structural timber and glued laminated timber – Determination of some physical and mechanical properties*. European Committee for Standardization.

EN 1611-1 (1999) + A1 (2002). *Sawn timber – Appearance grading of softwoods – Part 1: European spruces, firs, pines, Douglas fir and larches*. European Committee for Standardization.

EN 14081-1 (2016) + A1 (2019). *Timber structures – Strength graded structural timber with rectangular cross section – Part 1: General requirements.* European Committee for Standardization.

EN 14081-2 (2010) + A1 (2012). *Timber structures – Strength graded structural timber with rectangular cross section – Part 2: Machine grading; additional requirements for type testing.* European Committee for Standardization.
EN 14081-2 (2018). *Timber structures – Strength graded structural timber with rectangular cross section – Part 2: Machine grading; additional requirements for type testing.* European Committee for Standardization.
EN 14358 (2016). *Timber structures – Calculation and verification of characteristic values.* European Committee for Standardization.
EN 15497 (2014). *Structural finger jointed solid timber – Performance requirements and minimum production requirements.* European Committee for Standardization.
Fengal, D. & Stoll, M. (1973). *Variation in cell cross-sectional area, cell-wall thickness and wall layers of spruce tracheids within an annual ring*. Holzforschung, 27: 1 – 7.
Foley, C. (2003). *Modeling the effects of knots in structural timber*. Doctoral dissertation, Division of Structural Engineering, Report TVBK-1027, Lund Institute of Technology, Lund, Sweden.
Foslie, M. (1971). *Strength properties of Norway spruce. Part 3 – Strength properties of small defect free specimens.* The Norwegian Institute of Wood Technology, Report No. 42. (In Norwegian).
Galligan, W.L. & McDonald, K. A. (2000). *Machine grading of lumber – Practical concerns for lumber producers.* Forest Products Laboratory, General Technical Report FPL-GTR-7, Madison, WI, USA.
Gerhards, C.C. (1982). *Effect of moisture content and temperature on the mechanical properties of wood. An analysis of immediate effects.* Wood and Fiber Science, 14(1): 4 – 36.
Glos, P. & Heimeshoff, B. (1982). *Möglichkeiten und Grenzen der Festigkeitssortierung von Brettlamellen für den Holzleimbau*. In: Ingenieurholzbau in Forschung und Praxis (Ehlbeck und Steck). Bruderverlag, Karlsruhe, Germany. (In German).
Goodman, J. R. & Bodig, J. (1980). *Tension behaviour of wood – an anisotropic inhomogeneous material.* Colorado State University, Structural research report No. 32, Fort Collins, USA.
Hanhijärvi, A. & Ranta-Maunus, A. (2008). *Development of strength grading of timber using combined measurement techniques.* Report of the Combigrade-project – phase 2, VTT Publications 686:55.
Hankinson, R. L. (1921). *Investigation of crushing strength of spruce at varying angles of grain.* Air Service Information Circular, 3(259), Material Section Report No. 130, US Air Service, USA.
Havimo, M., Rikala, J., Sirviö, J. & Sipi, M. 2008. *Distributions of tracheid cross-sectional dimensions in different parts of Norway spruce stems*. Silva Fennica 42(1): 89 – 99.
Hoffmeyer, P. (1984). *Om konstruktionstreas styrke og styrkesortering.* In: *Skovteknologi. Et historisk og perspektivisk strejftog*. Dansk skovforening, pp. 34 – 46. (In Danish).
Hoffmeyer, P. (1990). *Failure of wood as influenced by moisture and duration of load.* Doctoral thesis, State University of New York, Collage of Environmental Science and Forestry, Syracuse, New York, USA.
Hu, M. (2018). *Studies of the fibre direction and local bending stiffness of Norway spruce timber.* Doctoral dissertation, Department of Building Technology, Report no. 307/2018, Linnaeus University, Växjö, Sweden.

Hu, M., Olsson, A., Johansson, M. & Oscarsson, J. (2018). *Modelling local bending stiffness based on fibre orientation in sawn timber.* European Journal of Wood and Wood Products, 76: 1605 – 1621.

Isaksson, T. (1999). *Modelling the variability of bending strength in structural timber – Length and load configuration effects.* Doctoral dissertation, Division of Structural Engineering, Report TVBK-1015, Lund Institute of Technology, Lund, Sweden.

Isaksson, T. (2003). *Structural timber – Variability and statistical modelling*. In: Thelandersson, S. & Larsen, H. J. (eds.) *Timber engineering*, John Wiley & Sons Ltd, Chichester, England, p.45–64.

Jenkel, C. & Kaliske, M. (2018). *Simulation of failure in timber with structural inhomogeneities using an automated FE analysis.* Computers & Structures, 207: 19 – 36.

Johansson, C.-J. (1976). *Tensile strength of glulam laminations – The effect of knots on tensile strength parallel to the grain in glulam laminations of Norway spruce.* Chalmers University of Technology, Internal report No S76:18, Gothenburg, Sweden. (In Swedish).

Johansson, C.-J. (2003). *Grading of timber with respect to mechanical properties*. In: Thelandersson, S. & Larsen, H. J. (eds.) *Timber engineering*, John Wiley & Sons Ltd, Chichester, England, p. 23–43.

Johansson, C.-J., Brundin, J. & Gruber, R. (1992). *Stress grading of Swedish and German timber – a comparison of machine stress grading and three visual grading systems.* SP Swedish National Testing and Research Institute, SP REPORT 1992:23.

Johansson, C.-J. & Claesson, T. (1989). *Hållfasthet och styvhet hos maskinsorterat virke. En studie av utfall från fem sorteringsmetoder.* SP Swedish National Testing and Research Institute, SP REPORT 1989:50.

Johansson, M. (2011). *Structural properties of sawn timber and engineered wood products*. In: Bergkvist, P. (ed.) *Design of timber structures*, Swedish Forest Industries Federation, Sweden.

Johnson, R. A. & Wichern, D. W. (2013). *Applied multivariate statistical analysis: Pearson new international edition.* Pearson Education Limited, London, England. ISBN: 978-1-292-02494-3.

Kandler, G., Füssl, J., Serrano, E. & Eberhardsteiner, J. (2015). *Effective stiffness prediction of GLT beams based on stiffness distributions of individual lamellas.* Wood Science and Technology, 49: 1101 – 1121.

Kantola, M. & Kähkönen, H. (1963). *Small-angle X-ray investigation of the orientation of crystallites in Finnish coniferous and deciduous wood fibres*. Ann. Acad. Sci. Fenn. A VI 137: 1 – 14.

Kantola, M. & Seitsonen, S. (1969). *On the relation between tracheid length and microfibrillar orientation measured by X-ray diffraction in conifer wood.* Ann. Acad. Sci. Fenn. 300: 2 – 10.

Kollmann, F.P. & Côte Jr, W.A. (1968). *Principles of wood science and technology. Part 1 – Solid wood.* Springer-Verlag, Berlin Heidelberg, Germany.

Lackner, R. & Foslie, M. (1988). *Gran fra vestlandet – Styrke och sortering*. Norwegian Institute of Wood Technology, Report 74. (In Norwegian).

Lucacevic, M., Füssl, J. & Eberhardsteiner, J. (2015). *Discussion of common and new indicating properties for the strength grading of wooden boards.* Wood Science and Technology, 49: 551 – 576.

Madsen, B. (1992). *Structural Behaviour of Timber.* Timber engineering Ltd, North Vancouver, British Columbia, Canada. ISBN 0-9696162-0-1.
Madsen, B. & Buchanan, A. H. (1986). *Size effects in timber explained by a modified weakest link theory.* Canadian Journal of Civil Engineering, 13(2): 218 – 232.
Matthews, P. & Beech, B., 1976. *Method and apparatus for detecting timber defects,* U.S.: Patent No. 3976384.
Müller, U., Gindl-Altmutter, W., Konnerth, J., Maier, G.A. & Keckes, J. (2015). *Synergy of multi-scale toughening and protective mechanisms at hierarchical bran-stem interfaces.* Science Report 5, 14522. doi: 10.1038/srep14522.
NOAA (National Oceanic and Atmospheric Administration) (2020). *Trends in Atmospheric Carbon Dioxide.* https://www.esrl.noaa.gov/gmd/ccgg/trends/. (Accessed 8 Jan 2020).
Nyström, J. (2003). *Automatic measurement of fiber orientation in softwoods by using the tracheid effect*. Computers and Electronics in Agriculture, 41:91 – 99.
Ohlsson, S. & Perstorper, M. (1992). *Elastic wood properties from dynamic tests and computer modeling.* Journal of Structural Engineering, 118(10): 2677 – 2690.
Olsson, A. & Oscarsson, J. (2014). *Three dimensional fibre orientation models for wood based on laser scanning utilizing the tracheid effect.* In: Proceedings of World Conference on Timber Engineering. Quebec City, Canada, August 10 – 14.
Olsson, A. & Oscarsson, J. (2017). *Strength grading on the basis of high resolution laser scanning and dynamic excitation: a full scale investigation of performance.* European Journal of Wood and Wood Products, 75: 17 – 31.
Olsson, A., Oscarsson, J., Serrano, E., Källsner, B., Johansson, M. & Enquist, B. (2013). *Prediction of timber bending strength and in-member cross-sectional stiffness variation on the basis of local wood fibre orientation.* European Journal of Wood and Wood Products, 71: 319 – 333.
Olsson, A., Pot, G., Viguier, J., Faydi, Y. & Oscarsson, J. (2018). *Performance of strength grading methods based on fibre orientation and axial resonance frequency applied to Norway spruce (Picea abies L.), Douglas fir (Pseudotsuga menziesii (Mirb.) Franco) and European oak (Quercus petraea (Matt.) Liebl./Quercus robur L.).* Annals of Forest Science 75(102).
Ormarsson, S. (1999). *Numerical analysis of moisture-related distortions in sawn timber.* Doctoral dissertation, Chalmers University of Technology, Gothenburg, Sweden.
Oscarsson, J. (2014). *Strength grading of structural timber and EWP laminations of Norway spruce – Development potentials and industrial applications*. Doctoral dissertation, Department of Building Technology, Report no. 170/2014, Linnaeus University, Växjö, Sweden.
Paakkari, T. & Serimaa, A. (1984). *A study of the structure of wood cells by X-ray diffraction*. Wood Science and Technology, 18(2): 79 – 85.
Persson, K. (2000). *Micromechanical modelling of wood and fibre properties.* Doctoral dissertation, Department of Mechanics and Materials, Lund University, Lund, Sweden.
Price, L., Sinton, J., Worrell, E., Phylipsen, D., Xiulian, H. & Ji, L. (2002). *Energy use and carbon dioxide emissions from steel production in China.* Energy, 27(5): 429 – 446.
Rais, A. & Van de Kuilen, J.-W. G. (2015). *Critical section effect during derivation of settings for grading machines based on dynamic modulus of elasticity.* Wood Material Science & Engineering, 12(4):189 – 196.
Ridley-Ellis, D., Stapel, P. & Bano, V. (2016). *Strength grading of sawn timber in Europe: an explanation for engineers and researchers.* European Journal of Wood and Wood Products, 74: 291 – 306.

RISE (Research Institutes of Sweden) (2019). *Consultative group for finger joint and machine / visually sorted structural timber*. Protocol from 29th of November, 2019, Borås, Sweden.

Ritchie, H. & Roser, M. (2020). *CO_2 and Greenhouse Gas Emissions.* https://ourworldindata.org/co2-and-other-greenhouse-gas-emissions. (Accessed 19 Feb 2020).

Saranpää, P., Serimaa, R., Andersson, S., Pesonen, E., Suni, T. & Paakari, T. (1998). *Variation of microfibril angle of Norway spruce (Picea abies (L.) Karst.) and Scots pine (Pinus sylvestris L.) – comparing X-ray diffraction and optical methods.* In: Butterfield, B.G. (ed.), *Microfibril angle in wood*: IAWA & IUFRO, Christchurch, New Zealand, p. 240 – 252.

Saranpää, P. (2003). *Wood density and growth*. In: Barnett, J.R. & Jeronimidis, G (eds). *Wood quality and its biological basis*. Blackwell Publishing Ltd, Oxford, England, p. 87 – 117.

Sarnaghi, A. K. & van de Kuilen, J.W.G. (2019). *An advanced virtual grading method for wood based on surface information of knots.* Wood Science and Technology, 53: 535 – 557.

Schajer, S. G. (2001). *Lumber strength grading using X-ray scanning*. Forest Products Journal, 51(1): 43 – 50.

Shigo, A.L. (1985). *How tree branches are attached to trunks*. Canadian Journal of Botany, 63(8): 1391 – 1401.

Simonaho, S.-P., Palvianien, J. Tolonen, Y. & Silvennoinen, R. (2004). *Determination of wood grain direction from laser light scattering pattern.* Optics and Lasers in Engineering, 41(1): 95 – 103.

SIS (Swedish Institute for Standards) 230120 (2010). *Nordic visual strength grading rules for timber.* Inter Nordic standardization, Swedish Standard Institute. (In Swedish).

Soest, J., Matthews, P. & Wilson, B. (1993). *A simple optical scanner for grain defects*. In: Proceedings of the 5th International Conference on Scanning Technology & Process Control For the Wood Products Industry. Atlanta, GA, USA, October 25–27.

Steffen, A., Johansson, C.-J. & Wormuth, E.-W. (1997). *Study of the relationship between flatwise and edgewise moduli of elasticity of sawn timber as a means to improve mechanical strength grading technology.* Holz als Roh- und Werkstoff, 55: 245 – 253.

Swedish Forest Industries (2020). *Sweden's forest industry in brief*. https://www.forestindustries.se/forest-industry/facts-and-figures/. (Accessed 8 Jan 2020).

Säll, H. (2002). *Spiral Grain in Norway Spruce*. Doctoral dissertation, Växjö University, Växjö, Sweden.

The Swedish Forest Agency (2020). *The Statistical Database.* https://www.skogsstyrelsen.se/en/statistics/. (Accessed 8 Jan 2020).

Thelandersson, S. (2003). *Introduction: Wood as a Construction Material*. In: Thelandersson, S. & Larsen, H. J. (eds.) *Timber engineering*, John Wiley & Sons Ltd, Chichester, England, p. 23–43.

United Nations (2015). *Paris Agreement*. https://unfccc.int/process-and-meetings/the-paris-agreement/the-paris-agreement. (Accessed 8 Jan 2020).

Viguier, J., Bourreau, D., Bocquet, J.-F., Pot, G., Bléron, L. & Lanvin, J.-D. (2017). *Modelling mechanical properties of spruce and Douglas fir timber by means of X-ray and grain angle measurements for strength grading purposes*. European Journal of Wood and Wood Products, 75: 527 – 541.

Worrell, E., Price, L., Martin, N., Hendriks, C. & Meida, L. O. (2001). *Carbon dioxide emissions from the global cement industry*. Annual Review of Energy and the Environment, 26: 303–329.
Åstrand, E. (1996). *Automatic Inspection of Sawn Wood*. Doctoral dissertation, Department of Electrical Engineering, Report no. 424, Linköping, Sweden.